1

State-of-the-Art Multi-Detector CT Angiography in Acute Pulmonary Embolism: Technique, Interpretation and Future Perspectives

IJC Hartmann, PJ Abrahams-van Doorn
and C Schaefer-Prokop
Erasmus MC University Medical Center Rotterdam,
Meander Medisch Centrum Amersfoort
The Netherlands

1. Introduction

Since the first application of CT angiography (CTA) for the diagnosis of acute pulmonary embolism (PE) in the early nineties (1), CTA has become the first imaging technique of choice in the workup of patients with suspected PE.

Though the considerable inherent limitations of CTA with single-detector CT (SDCT) systems, its diagnostic potential for direct visualization of arterial clots was instantaneously appreciated by the radiological community. Limited by a maximum breath hold of 30 s and a single detector row data acquisition, image quality and thus diagnostic efficiency was limited by the trade off between the need to cover a certain scan length and the spatial resolution determined by the slice collimation: e .g., with a slice collimation of 5 mm only a scan range of 15 cm could be covered within 30 s. Even with use of 3 mm collimation and a pitch of 1.7, a confident detection of acute PE was only possible down to the segmental level.

With the newest generation CT scanners the full chest can be scanned in less than 4 s with sub-millimeter collimation which has become the standard nowadays (see table 1). Small thrombi can be identified in subsegmental arterial branches and elaborate post-processing techniques can be executed, resulting in a significant increase of both sensitivity and specificity in PE detection. This substantial gain in image acquisition speed and spatial resolution also lead to novel image interpretation concepts including the assessment of perfusion defects of the lung parenchyma and the evaluation of cardiac dysfunction, both of which are important determinants for the clinical outcome of the patient.

Besides the significant increase of detectors in the most recent generations of CT scanners a complete novel concept has been developed: dual-source CT. Although the main gain of the use of two radiation sources is the steep increase in temporal resolution, which is especially of benefit for cardiac scanning, this new technique can also be used for PE detection by performing either a dual-source CT protocol resulting in CTA and CT perfusion datasets obtained during one image acquisition, or as a fast track protocol resulting in a dataset obtained within 1 s and without disturbing breathing artifacts, even in very dyspnoeic patients.

The development of faster CT scanning techniques has resulted in a substantial decrease of the percentage of non-interpretable scans (overall from 10% using SDCT techniques to up to 6% for multi-detector CT (MDCT)) (2, 3). However, the very fast data acquisition in a few seconds carries also new risks and new down-sides such as scans with suboptimal image quality due to a sub-optimal contrast medium injection protocol or a sudden Valsalva maneuver by the patient almost inevitably resulting in inadequate vessel enhancement. An examination with suboptimal quality and, as a result, ambiguous or completely impossible interpretation, is still the most important drawback of CT in the workup of patients with suspected PE. Many of these qualitatively suboptimal CT scan results can be avoided when acquisition and contrast medium injection protocols are optimized and proper patient instruction is executed, with special attention to specific subgroups such as ICU and pregnant patients. Furthermore, interpreters of the CT datasets should be familiar with a good interpretation protocol taking benefit of the appropriate post-processing techniques and should keep in mind the potential pitfalls.

In the following, we will focus on the optimization of CTA protocols using most modern MDCT systems, with special attention to the acquisition and contrast medium injection techniques and with potential adaptation of these protocols for specific patient subgroups. On the other hand, we will discuss options for display optimization of the datasets using post-processing techniques and recently developed computer aided detection (CAD) systems. Finally potential pitfalls, related to the technique, the patient and the interpreter will be explained.

2. Image acquisition protocols

2.1 Scanning parameters

Due to the continuous and rapidly advancing MDCT technology, scanning protocols need to be continuously adapted, too (table 1). The optimal scan protocol depends on the generation of scanner (e.g., the number of detector rows being used) and the vendor of the CT machine. Using MDCT scanners with ≥ 16 detector rows, the scan time is reduced to < 10 s, resulting in a significant decrease of movement artefacts and an increase in spatial resolution, obviating an adaptation of the scan protocol even in very dyspnoeic patients. Therefore, the use of CT scanners with less than 16 detector rows cannot be advocated anymore for obtaining CT pulmonary angiography (CTPA).

Scanner type (number of detector rows)	**Collimation** (mm)	**Rotation time** (s)	**Scan duration** (s, 24 cm)
4	1-1.25	0.5	≤ 20
4 (dyspnea)	2-2.5	0.8	≤ 10
16	0.625-1	0.37-0.42	≤ 8
64	0.5-0.625	0.35-0.42	≤ 4
128	0.6	0.30	< 3
128 DS	0.6	0.28	< 1
256	0.625	0.33	< 2
320 (160)	0.5	0.35	< 4

DS = dual source, 320 detector snap shot imaging, 160 detector row spiral data acquisition

Table 1. Scan parameters for the different types of scanners.

2.2 kV and mAs

Lowering the kV from 120-130 kV to 100 kV or even 80 kV substantially decreases radiation dose roughly up to 60% (4-7). The resulting increase in image noise is compensated by the improved absorption of iodine with lower kV resulting in higher HU of the enhanced vessels. Several studies could show that visualization especially of small vessels was improved with lower kVp (8).

This 80 kV scanning technique, however, can only be applied in patients weighting less than 75 kg (7). In large patients (body weight > 90 kg) and in patients of whom the arms cannot be brought above the head (e.g., in ICU patients), lowering the kV usually results in such an increase in image noise that image quality is substantially decreased and diagnostic quality not guaranteed anymore.

The use of dose modulation software should be routinely used. Dose modulation techniques as offered by all manufacturers modulate the mAs as function of the body dimension along the xy-axis and along the z-axis of the patient. That way data are acquired with lowered dose during the mid part of the chest as compared to the upper thoracic inlet at the level of the shoulders and the lower thoracic outlet, where the liver is already included into the scan. Similarly radiation is lowered for ventro-dorsal transmission direction as compared to the right-to-left direction. These techniques are quite effective with a dose reduction of up to 50% in the chest (9, 10), however, depending on the dose level originally determined by the 120 kVp and the region of the chest, e.g., shoulders central part, thorax outlet/upper abdomen. Further dose reduction is possible by lowering the kV as function of body weight and body dimensions. In table 2, a guideline is provided for the adaptation of kV and reference mAs to the body weight of the patient.

Weight	kV	mAsref
<50 kg	80	1.5 mAs/kg
50-70 kg	100	120
70-90 kg	100(120)	150
>90 kg **	120	150

** kVp may not be lowered in patients which are scanned with arms along the body.

Table 2. Dose protocols adapted to the patient's body weight.

A low signal-to-noise ratio may deteriorate the image quality significantly, impeding a reliable interpretation of especially the subsegmental and more peripherally located pulmonary arteries. This may cause diagnostic problems in obese patients. Therefore, in patients > 120 kg image quality may be further improved by using slower rotation times to increase the amount of delivered dose. Also reconstruction of thicker slices (e.g., 2 mm instead of 1 mm) may be helpful to allow a more meaningful interpretation of too noisy images.

2.3 Dose aspects

The radiation dose of a CTPA is described in DLP (in mGy x cm) which takes into account the individual scan length. It is calculated using the equation: dose-length product (DLP) = scan length x $CTDI_{vol}$. The resulting effective dose *E* (in mSv) is calculated using the specific conversion factor of 0.014 (11) or 0.017 (12) mSv per mGy x cm for a CTPA covering the whole chest. For simplification, the conversion factor is the same for men and women, although the individually received dose is higher for women because of radiation to the breasts. The $CTDI_{vol}$ is given on the scanner console after each examination. As a rule of

thumb it can be said that for a total CTPA with a scan length of 30 cm the effective dose amounts to about 40% of the $CTDI_{vol}$ for men and to about 50% of the $CTDI_{vol}$ for women.
If the scan range is reduced, the effective dose decreases proportionally. As a consequence, effective dose may vary substantially despite the fact that the same mAs and kVp settings have been chosen. The European Guidelines for Quality in Computed Tomography EUR 16262 suggest a maximum effective dose level for the chest of 9 mSv. In our experience, the required dose levels are lower and the $CTDI_{vol}$ does not exceed 5-7 mGy in a standard size patient (70 kg, 170 cm).
Lowering the kV has the important advantage of considerably decrease radiation dose for the patient. The absorption of iodine increases with lower kVp resulting in higher intravascular enhancement (figure 1). This effect can be used to compensate for the higher image noise resulting from lowering the kV. This increased noise is the reason that lowering the kVp is only recommended for children and low to normal weight persons but not in patients > 75 kg (7), unless the tube current is increased to keep the image noise constant. In slim patients and children, use of an 80 kVp protocol (without adaptation of the tube current) decreases the radiation dose to as low as 1.5-2 mSv.

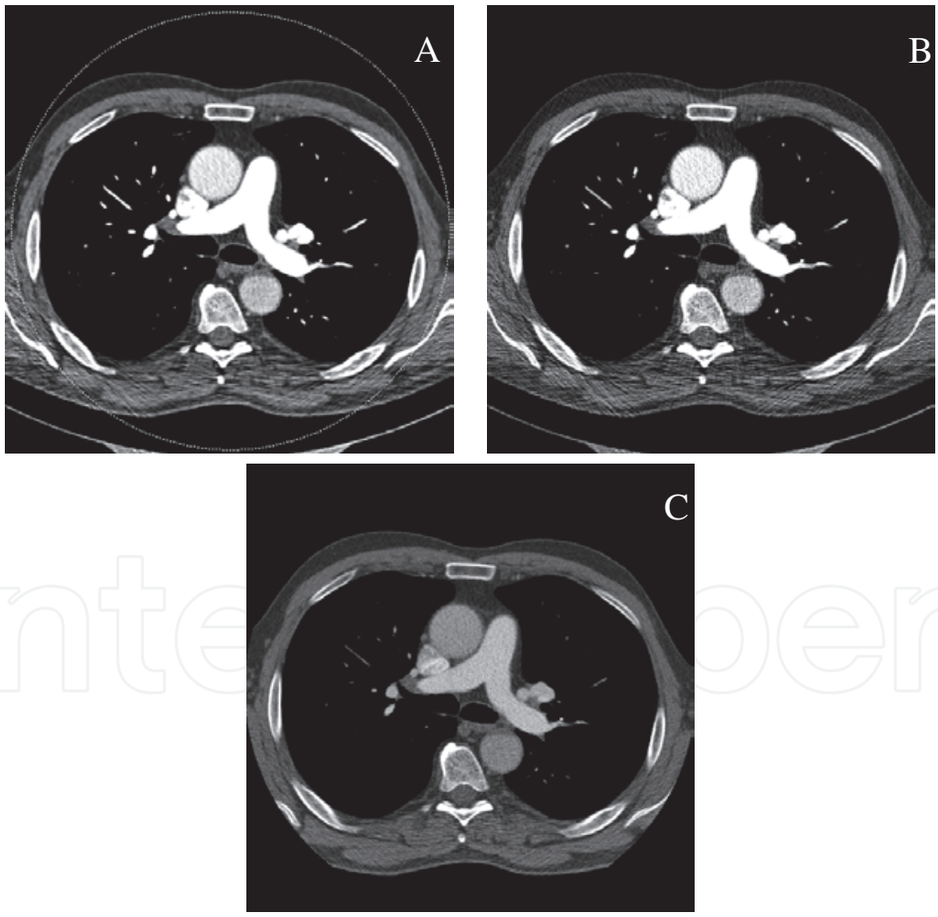

Fig. 1. Dual-energy CT of a 46-year-old male patient with acute PE, performed with 75 mL contrast medium with 400 mg/mL iodine concentration injected at 5 mL/s.
Axial 1-mm virtual 120 kV slice (A), 2-mm 80 kV slice (B) and 2-mm 140 kV slice (C), with mean contrast enhancement at the main PA of 541 HU, 709 HU and 284 HU, respectively.

In a recent study, comparing simulated low-dose CT scans, generated by the superimposition of computer-calculated noise, to a reference standard of 90 mAs in non-obese patients found no statistically significantly differences in the visualization of peripheral PE and inter- and intraobserver agreement (13).

2.4 Scan length and direction

The first CTPA protocols proposed a scan range between 2 cm above the aortic arch to 2 cm below the pulmonary veins. This protocol allowed for coverage of the central part of the lung with an appropriate spatial resolution at the time of slower data acquisition within a single breathhold. Today the whole chest can be easily covered within less than 5 s. Therefore, it becomes more important to pay attention to determine just the scan range needed without including too much of the neck or the upper abdomen to avoid unnecessary radiation. This seems to be especially important in young patients and in women. Though retrospective data analysis did not find a diagnostic disadvantage for determining or excluding PE if the lung tops and the lower costophrenic angles are spared (14) , this approach is not generally advocated but should be reserved to certain indications such as repeat examinations in young patients. It may lead to loss of information with respect to alternative diagnosis (e.g., extent of pleural effusion or pneumonia) and is therefore not considered useful in elderly patients or in patients with known or suspected comorbidity. This approach also seems to be less well definable within a standardized protocol that ideally should be the same independent of institutional, personal or time related effects.

With SDCT, a caudo-cranial scanning direction was in general preferred as breathing artefacts are less disturbing in the upper lung zones and to avoid beam hardening artefacts due to inflow of high density contrast medium. With shorter scanning times and use of a saline chaser bolus these issues have been overcome. Today, both caudo-cranial and cranio-caudal scanning directions are in use, depending on local preference.

2.5 ECG-gating

There are three potential indications why to obtain a CTA data set with ECG-gating, though all three of them have not yet found their way into clinical routine or have not been found to provide substantial advantages. Limiting factors for ECG-gated CTPA protocols are the increase of radiation dose and the prolongation of scan time.

a. Prospective ECG-gating diminishes motion artefacts due to cardiac pulsation, especially in the lingula and left lower lobe vessels. As a result, it may improve image quality as compared to non-ECG-gated CTPA. Whether ECG-gated CTPA indeed results in a clinically relevant increase of diagnostic accuracy remains questionable and studies on this topic are so far not available. Up to now, ECG-gating has not found its way into clinical routine in the workup of patients with potential PE (15).
b. The role of ECG-gated data acquisition may be more important in the context of the assessment of cardiac function rather than image quality. ECG-gated CTPA allows for functional assessment of the right ventricle (RV). Dysfunction of the RV has been proven to be an independent predictor of survival in patients with PE. Yet, assessment of the RV/LV (right ventricle / left ventricle) ratio on non-ECG-gated scans were found to equally well assess RV dysfunction as functional parameters based on ECG-gated CTPA, and
c. a triple or dual rule-out protocol to assess the presence of PE, coronary disease or aortic dissection in patients with acute chest pain, requires ECG-gating to obtain the necessary quality for the evaluation of coronary arteries (16).

2.6 Injection protocol

The injection protocol should be optimized to ensure a constant and high degree of pulmonary arterial enhancement during the complete data acquisition. A minimal attenuation of 300 to 350 HU (i.e., 250 to 300 HU net contrast enhancement) is considered optimal for the assessment of PE at CTPA (17, 18). Suboptimal vascular opacification is a major reason for non-diagnostic scans and further aggravates other artefacts such as partial volume effects or movement artefacts potentially causing false positive interpretations.

Optimizing the injection protocol becomes more challenging the shorter the scan time is, as Valsalva maneuvers or inadequate scan delay time can completely destroy the whole scan.

The most important causes of general insufficient enhancement are: low injection rate, wrong bolus timing and decreased heart function. All these causes are in a way predictable and measurable and therefore can be overcome by appropriate steps.

1. A sufficiently high delivery of mg iodine per s should be obtained by choosing a high flow injection rate (4 – 6 mL/s) and/or a high concentration of the contrast medium (370-400 mg of iodine/mL). This will result in good visualization of small, peripherally located pulmonary arteries, eventually improving the overall sensitivity (19). Similarly as with radiation, more iodine is needed in large patients to achieve a comparable opacification of the pulmonary arteries as in a small patient. This can be achieved by either increasing the iodine flow rate (20) or by increasing the total volume of administered contrast medium (21) to overcome the inversely proportional relationship between opacification of the pulmonary arteries and body weight (17).
2. The duration of contrast medium injection should approximately be equal to the sum of the scan duration and the delay time. For very short scan durations, the delay time has to be increased. After reaching the trigger threshold 5-8 s of delay have to be added depending on the type of scanner (the faster the scanner and the shorter the acquisition time, the more delay time should be added). Importantly, if for some reason the injection time is increased, e.g., due to limited venous access, the scan delay has to be prolonged accordingly to avoid scanning and data acquisition when pulmonary arteries are not yet sufficiently opacified (22). The trigger level and the region of interest chosen for bolus triggering have to be chosen to allow for adequate contrast build-up down to the peripheral arteries during the complete scan acquisition (table 3). If scanning is started too early, especially in very fast high-end MDCT scanners, inhomogeneity in opacification can result in pseudo-filling defects. Narrowing the window settings is helpful to differentiate between pseudo-defects and true PE.

   As a consequence, contrast volume can be substantially reduced for CTPA with fast high-end scanners.

Scan duration (s)	**Scanner type**	**With saline** (ml) / (ml/s) / (s)	**Without saline** (ml)
≤ 5	16, ≥ 64	70 + 40 / 5 / 8-10P*	80
10	4 (dysp.), 16	80 + 40 / 5 / 5-8P*	100
20	4	100 + 40 /4 /5P*	120

* P is the time that should be added after a threshold of 150 HU is reached using bolus triggering. The region of interest (ROI) is placed in the pulmonary trunk.

Table 3. Injection protocols for the different types of scanners.

3. Frequently, a saline chaser of 30-60 mL is used. It is immediately injected with the same injection rate after the contrast medium bolus.
   The advantages of such a saline flush are threefold:
   a. it flushes the contrast medium out of the subclavian vein and superior vena cava (SVC), decreasing the risk of beam hardening artefacts. These artefacts are more frequently seen with use of high concentration and/or high flow rates and hamper the visualization of the right pulmonary artery and its branches in the right upper lobe.
   b. it prolongs the length of the contrast plateau resulting in a more homogeneous intravascular contrast, and
   c. finally, it decreases the total volume of contrast medium needed (23).
4. With the short and very short scanning times that result from the use of modern MDCT scanners, an individualized injection timing using bolus triggering has become essential. It compensates for unexpected changes in circulation time, which can be slowed down due to right-sided heart failure, pulmonary hypertension (PH) or low cardiac output, or on the other hand can be increased in case of a hypercirculatory status e.g., in adolescents or pregnant women.

The ROI for bolus triggering is usually localized in the pulmonary trunk or pulmonary artery (PA) but may as well be set in the RV or the ascending aorta. The preset trigger level is usually between 150 and 200 HU.

The right cubital vein is the preferred site for contrast medium injection in CTPA to avoid streak artefacts caused by the nearly horizontal course of the left brachiocephalic vein. In general, both arms are placed above the head. Some authors prefer positioning the left arm above the head and the right arm parallel to the body with right-sided contrast medium injection as this technique reduces the risk for hampered inflow of contrast medium due to compression of the brachiocephalic vein at the level of the thoracic inlet. As a consequence of placing the arm aside the body, however, the image noise in the scanned volume may increase especially when low-dose protocols are used.

In a subgroup of patients with suspicion of PE but contraindications for iodinated contrast medium injection, gadolinium may be used as an alternative to iodine containing contrast medium (24, 25). Diagnostic CTPA with adequate opacification of the complete pulmonary arterial tree up to the subsegmental level using gadolinium can only be obtained with fast data acquisition (MDCT with ≥ 16 detector rows) as the amount of gadolinium than can be injected for CTPA is limited to 0.3-0.4 mmol/kg. A high injection rate protocol has to be chosen also with gadolinium. As it is well known, gadolinium is contraindicated in patients with severe renal insufficiency and up-to-date guidelines for its use have to be followed (ESUR guidelines on contrast media; www.esur.org).

2.7 Filtered back projection and iterative reconstruction

Filtered back projection is currently the standard technique to reconstruct the image dataset from the raw scan data. Iterative reconstruction techniques are an alternative method to work with the raw data whereby image data are corrected using several different models. Iterative reconstruction is routinely used in PET and SPECT imaging. These techniques reduce image noise while preserving sharpness, which is especially useful in using low-dose CT protocols. In addition, the use of iterative reconstruction further improves image quality

by reducing artefacts, i.e., spiral artefacts and beam hardening artefacts, the latter might be especially advantageous in the assessment of use of dual-energy CT (DECT) perfusion images (see below under 'Dual-source CT'). So far, these techniques were not used in CT as the algorithm requires significant computational time. Due to modification of the technique and the increased speed of processing, this technique has now become available in routine clinical practice for CT. A potential disadvantage of this technique may be a different image appearance, of which the potential effect on the detection of PE has so far not been studied. Whether the decrease of image noise by iterative reconstruction resulting in image quality improvement in low-dose CTPA protocols will balance the potential disadvantage of the different aspect of the structures at CT needs to be subject of further study.

2.8 Dual-source CT

Dual-source CT (DSCT) scanners can be used in two different ways for the detection of acute PE. Using the "Flash" technique, the chest can be scanned from the apex to the diaphragm with the thinnest collimation in less than 1 s. This will further reduce the risk for movement artefacts and increases the temporal resolution.

Alternatively, DSCT scanners offer the option to reconstruct "material specific images", e.g., images in which the distribution of iodine in the lung parenchyma is used to produce lung perfusion images (27-30). In DECT, lung perfusion does not correspond to blood flow analysis in its strict definition, but refers to the iodine enhancement at one point in a time (blood volume), which is related to the pulmonary blood flow or microcirculation of the lung. The distribution of the iodine within the pulmonary capillaries is influenced by various parameters such as the amount of contrast medium administered and the anatomic structures the contrast medium passes through, both, before and after the pulmonary capillary bed (31).

There had been attempts earlier to produce lung perfusion images using single-source CT scanners: They used dynamic scan protocols or assessed parenchymal density by means of color coded maps. Since these techniques have serious limitations, they never found their way into broad clinical application. Using the dynamic technique, additional serial scanning has to be performed with a rather limited coverage. Subtracting an enhanced from an unenhanced scan will further increase display of lung perfusion but requires a very long breathhold (to obtain both scans within one breathhold) and still suffers from subtraction artifacts.

These limitations could be overcome by dual-source / dual-energy CT technique. Using DSCT with dual-energy technique, two datasets obtained at two different kilovoltages are reconstructed. Fusion of the two image sets with an 80:140 kVp linear weighting of 0.3- 0.4 produces a "standard" CTA of 120 kVp (figure 2). Subtracting the lower kV from the higher kV images using dedicated processing software produces CT-perfusion colour-coded maps, resembling the distribution of iodine in the lung. The 80 kVp data set, although it suffers from an increased image noise, the contrast to noise ratio is optimised (see above under 'kV and mAs ') and therefore may be helpful for the assessment of PE in peripheral pulmonary arteries. To allow the contrast material to perfuse the complete lung, the delay time should not be too short (see below) and a saline flush is needed to limit streak artefacts from the SVC. The latter may be further reduced by using a split-bolus injection technique (32).

There are a number of new pitfalls in these perfusion images such as gravity dependent perfusion, pseudo/high perfusion due to dense contrast material in the thoracic veins, cardiac motion, or artefacts caused by underlying pulmonary disease especially emphysema and the reader has to become familiar with them when assessing CT perfusion images (33). Recent studies in small patient groups have found a good correlation between pulmonary perfusion defects seen by DECT perfusion imaging and the gold standard, pulmonary perfusion (SPECT) scintigraphy (34, 35).

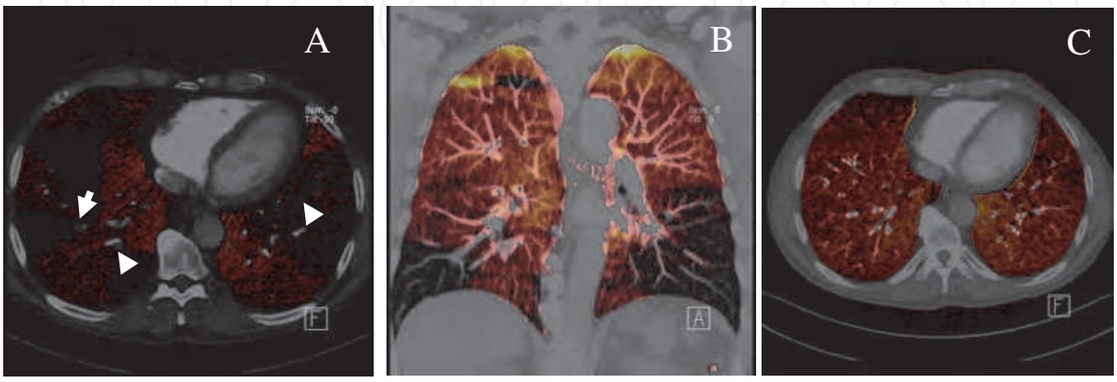

Fig. 2. Dual-energy CT of a 46-year-old male patient with acute PE. Fused color-coded and virtual 120 kV axial images (A) and coronal MPR (B) showing bilateral multiple segmental and sub-segmental thrombi (white arrows) obstructing the pulmonary arteries. As a result, multiple (sub) segmental perfusion defects are observed (black areas). A follow-up scan after 6 months of anticoagulant treatment revealed neither residual thrombi nor perfusion defects (C).

The disadvantage of the first generation DSCT scanners caused by a too small diameter of the field of view of the second tube (26 cm), resulting in incomplete truncated iodine maps in large patients, is now overcome in the second generation of DSCT scanners that provide a sufficient coverage also of the second tube (33 cm).
Besides the analysis of the distribution of iodine in the lung parenchyma, dedicated software algorithm visualizing the iodine content in the pulmonary vessels has been developed. This software was designed especially to differentiate true PE from other causes of low HU values such as low contrast enhancement and partial volume effects, especially in small pulmonary vessels. A first evaluation of this technique demonstrated that this algorithm may especially be helpful in the exclusion of PE (36).
Summarizing it can be said that although the perfusion technique seems promising for combining direct visualization of the thrombus with the functional consequences, namely perfusion defects (figure 1). The radiation dose of DECT technique is equivalent to or slightly higher than for the single tube CT technique, but the potential benefits of DECT are thought to balance the possible minor dose increase. However, the actual additional value of this technique for diagnosis, prognosis and therapy monitoring still needs to be determined in future studies.

2.9 Patient instruction

It is generally recommended to perform image acquisition for a CTPA during breathhold and in inspiration.

Breathing artefacts and a Valsalva maneuver by the patient hampering contrast-inflow are still major causes for sub-optimal scan quality. A careful patient instruction by the technologist is therefore very important: it should include an appropriate explanation of the effects of fast contrast-inflow (transient feeling of warmth and unusual oral taste), a performance of a trial breathhold for the required scan duration and a careful explanation not to increase intrathoracic pressure by a Valsalva maneuver. By watching the movement of the abdominal surface adequate suspension of respiration can be assessed. Patients usually require about 4 s between the breathhold command and the actual scan to obtain a full inspiration. Substantial movement artefacts may occur if scan delay is too short or patients are improperly instructed. In the elderly even more than 4 s may be needed. Individual instruction by the technologist instead of using the automatic command and start of scanning further reduces the chance of significant breathing artefacts. With slower CT scanners and scanning times of more than 15 s (below 16-row CT scanners) a short hyperventilation of 3-4 times before starting the data acquisition may be helpful to ensure breathhold capability.

Deep inspiration immediately prior to the image acquisition may lead to transient interruption of the contrast column in the pulmonary arteries. This is the result of variable inflow of non-opacified blood from the inferior vena cava as a normal response to the negative intrathoracic pressure (26). Valsalva maneuvers on the other hand, lead to diminished inflow of contrast medium as a result of increased intrathoracic pressure. Both may lead to inhomogeneous or inadequate contrast enhancement of the pulmonary arteries that becomes even more critical with faster scanners that require less than 5 s for full data acquisition. Some authors have therefore recommended obtaining CTPA in expiration (to avoid inflow of uncontrasted blood via the inferior vena cava). The disadvantage of crowded and compressed vascular structures in expiration and the substantially lowered display quality of the lung parenchyma, however, make this a technique that cannot be generally recommended. Some patients tend to 'gasp for air' internally against a closed glottis at the end of scan acquisition. This may result in motion artefacts due to the involuntary diaphragmatic movements and can also be avoided by careful patient instruction.

In severely dyspnoeic patients, shallow breathing is preferred over forced breathholding to avoid severe and uncontrollable movement artefacts. This will slightly reduce the quality of both the axial slices and multiplanar reformats (MPR's), but in the majority of cases a diagnostic scan can be obtained, at least of the central pulmonary arteries.

2.10 CTPA during pregnancy

Venous thrombo-embolic disease has a two- to fourfold increased incidence during pregnancy and is a leading cause of maternal mortality. Ultrasound of the leg veins has been advocated as the first clinical test for suspected non-life threatening thrombo-embolism (Statement of the Fleischer Society) because further radiographic imaging is only required if leg ultrasound is normal (37).

The question which technique to use next for pregnant patients with suspected thrombo-embolism has been hotly debated (38-41). There is no general consensus to which diagnostic technique is the most appropriate to diagnose acute PE in pregnant women. It is important to know that at no time point of the pregnancy (including the first three months) a CTPA delivers a radiation dose that poses a risk to the unborn child, and risks of an undiagnosed PE are much greater than any theoretical risk to the fetus from diagnostic inaging (42, 43).

Since diagnosis of a deep venous thrombosis represents a sufficient indication for treatment, the first diagnostic step should be an ultrasound examination of the deep leg veins. For evaluating the pulmonary arteries, a CTPA or a perfusion scintigraphy can be obtained. The latter is only useful if the chest radiograph excludes overlying parenchymal disease. The absorbed dose to the uterus (and fetus) is approximately 0.2-0.3 mGy for ventilation / perfusion imaging but varies dependant on the agents used (44). Recent estimations of the radiation dose absorbed by the fetus during CTPA have been reported to be as low as 0.026 mSv using SDCT and 0.014 mSv for MDCT (45).
More concern has been devoted to an increased risk of cancer induction after radiation exposure during CTPA to radiosensitive organs in pregnant patients, particular breast tissue. The calculated breast dose using organ-specific conversion factors have been calculated to range between 5.5-13.1 mGy (average 7.4 mGy) per breast. An exposure of 10 mGy to the breasts of a woman aged 35 years increases the risk of breast cancer by approximately 14% over the background rate for the general population (46). A perfusion scintigraphy provides less dose for the breasts at the expense of a slightly increased dose for the foetus especially since the radiopharmacon is eliminated through kidneys and bladder.
If a CTPA examination is planned to be carried out, it is important to adapt the protocol to reduce dose and to optimize contrast application.
As previously described the kV should be reduced to 100 kV, in very small patients to 80 kV to substantially reduce radiation dose. The scan range should be sharply limited to the lung parenchyma. Further on, the pitch and slice collimation can be increased to further reduce dose (pitch of 1.7-2 and slice thickness of 1-1.5 mm). Since pregnant women have a hypercirculatory state with increased cardiac output and increased plasma volume already at an early state of their pregnancy, the injection rate should be increased to 6 ml/s to ensure adequate vascular enhancement (47).
To avoid a valsalva maneuver in these usually very nervous patients, patients should be instructed to breath shallowly instead of holding their breath.
Last but not least, it seems to be the most important to obtain an examination of interpretable image quality that justifies the radiation given to patient and child. Thus per institution, that technique should be chosen for which interpretation experience and technical standard are highest.

2.11 ICU patients

In patients under respiratory ventilation the quality of a CTPA is highly dependant on the capacity of cooperation of the patient. If the scan quality is likely to be substantially improved when image acquisition is performed with full sedation of the patient and in full inspiration, it should be discussed with the clinicians before obtaining the scan. Such a procedure and dependant on the scanner type, it might require an interruption of the respiratory ventilation for a period of 15-20 s which poses no problem in most patients. When apnea during image acquisition is not an option, the frequency of ventilation can be reduced in order to minimize breathing artefacts.
In addition, as patients are frequently scanned with their arms parallel the body, the scan has to be obtained with a sufficiently high dose to ensure low noise and adequate signal (lowering kV and mAs is not an option in this patient group).

2.12 Repeating CTPA

Despite the use of an optimized protocol and careful patient instruction, the CTPA may still result in a non-diagnostic scan. One should only consider repeating the examination if a better

result can be expected after adequate adaptation of the protocol or patient preparation, e.g., having a better venous access available, adapting contrast medium injection rate or dose, choosing a longer scan delay, or changing patient instruction (figure 3).

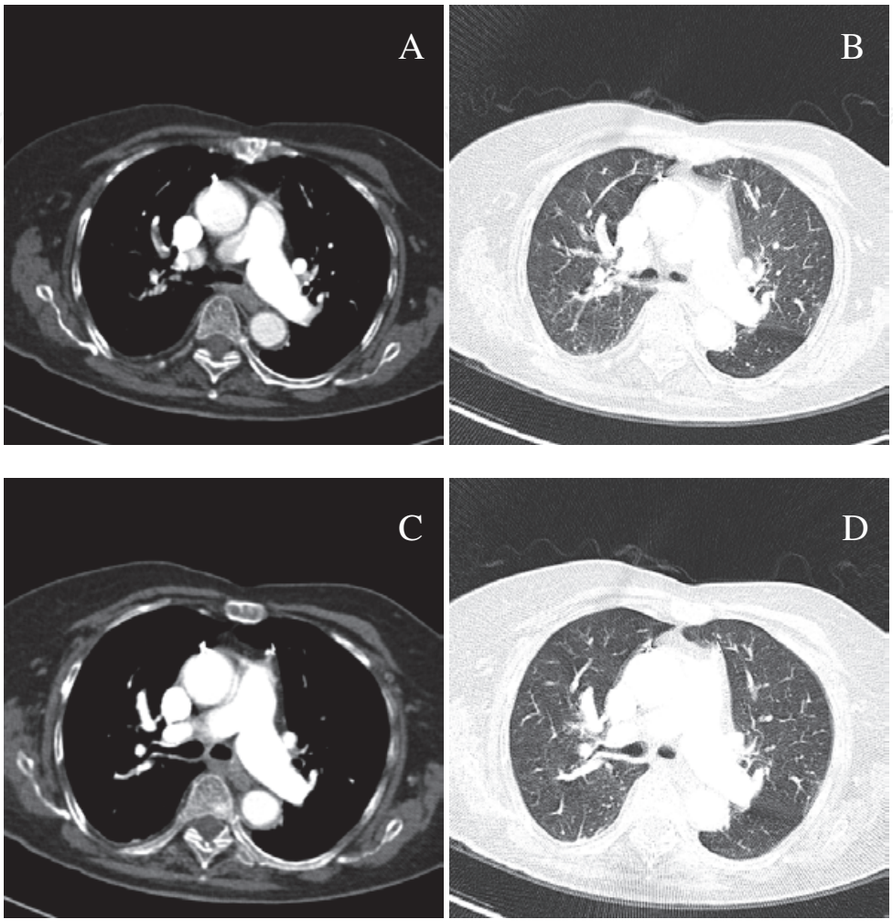

Fig. 3. CTPA of a 61-year-old female patient with severe dyspnea. The 1-mm axial slices in mediastinal (A) and lung parenchyma (B) window setting demonstrate severe breathing artefacts resulting in a non-interpretable scan result. The CTPA was repeated immediately after the first acquisition with a second contrast medium bolus injection, which resulted in a CTPA of diagnostic quality (C and D).

2.13 Thrombus load and right ventricular function: predictors of adverse outcome?

Besides diagnosing PE by direct visualization of the thrombus, a CTPA can also be helpful in predicting the outcome of patients with PE, which is assumed to be related to clot burden and RV function (48).

Several parameters in predicting right ventricular dysfunction (RVD) have been mentioned, like the RV/LV ratio, dilatation of the PA, SVC and azygos vein, bowing of the interventricular septum and the pressure in the right atrium. Of these, only a RV/LV ratio ≥ 0.9-1.5 obtained on the axial views has been shown to be directly correlated with RVD and adverse outcome (49).

For the quantification of thrombus load in the pulmonary vascular tree, several scoring systems have been proposed. The modified Walsh and Miller scores, which were primarily angiographic scores, but adapted to the needs of CT, both quantify the severity of PA obstruction (50). The CT derived scores proposed by the groups of Qanadli and Mastora not only give information about thrombus load, but also about the degree of obstruction (51, 52). However, despite the excellent clot imaging, the literature still shows contradicting results in the usefulness of the PA obstruction index as a predictor of RVD or short-term survival. Furthermore, since obtaining these scores is very time-consuming they have never found their entrance in clinical routine so far. The use of CAD software might overcome this limitation in the future (37).

3. Interpretation of CT: How it should be done

3.1 Slice reconstruction

Dependant on the slice collimation used during acquisition, slice reconstruction width varies from 0.9 to 1.5 mm, preferably 0.9-1.0 mm. Usually an overlapping reconstruction algorithm is applied with a reconstruction index of 0.7-1.0. Thinner slice thicknesses do not further contribute to the diagnosis and will unnecessarily decrease signal-to-noise ratio. In obese patients, a smoothing reconstruction algorithm and thicker slices of 1.5 or 2.0 mm might be advantageous to increase the signal to noise ratio. It is not recommended to use a slice thickness thicker than 2.0 mm to ensure optimal evaluation of peripheral pulmonary arteries (figure 4).

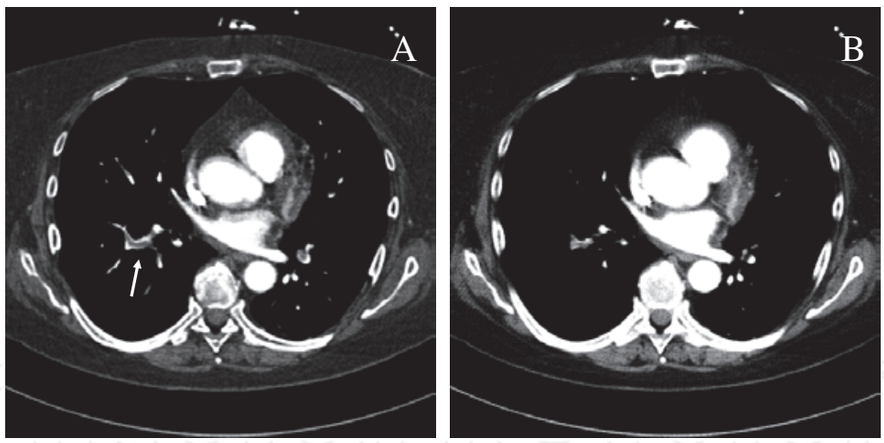

Fig. 4. CTPA in a 56-year-old female patient with progressive dyspnea. Axial 1-mm reconstruction revealing a PE in a subsegmental vessel surrounded by contrast medium (white arrow), a so-called 'railway track sign' (A), which is less well depicted on the 5-mm reconstruction (B).

3.2 Windowing

Axial slices in both soft tissue window setting (window width, WW = 400 HU; window level, WL = 30 to 40 HU) and pulmonary parenchyma window setting (WW = 1500 HU; WL = -800 to -600 HU) represent the base for diagnostic interpretation. When only fixed standard soft tissue window settings are used, especially in combination with a high iodine injection rate, small PE may be obscured by the dense contrast medium and may be

consequently missed. Therefore, the use of a modified relatively wide soft tissue window (WW = 700 HU; WL = 100 HU) has been proposed by some authors. Alternatively, an individual adaptation of the window setting can be applied that is flexibly adapted to the degree of vascular enhancement and vascular size: the WW is set slightly lower than twice the mean attenuation in the pulmonary trunk and the WL is set at about half of the mean attenuation of the pulmonary trunk (53).

A poor vascular enhancement is more difficult to overcome as the density difference between the opacified vessel and the thrombus is decreased. In this case, narrowing the window width and lowering window level settings may help to obtain a more confident diagnosis.

Although soft tissue window settings are necessary to provide direct visualization of intravascular contrast defects and thus provide the base for diagnosis, pulmonary window settings are also indispensable for the assessment of movement artefacts, which result in endovascular contrast inhomogeneities which may mimic pulmonary thrombi. The pulmonary parenchyma window setting is also important to differentiate pulmonary arteries from mucus filled bronchi and from venous structures that may not be opacified in an early scan phase (no accompanying bronchial structure).

The simultaneous assessment of either standard or adapted soft tissue window setting and pulmonary parenchyma window setting (e.g., on two monitors side to side or by toggling) will shorten the interpretation time and will potentially reduce false positive findings.

3.3 Image interpretation

An interactive cine mode interpretation on either a dedicated work station or using the PACS workstation is warranted to assess the large number of slices, usually 300-450 slices for a multi-detector CTA. The magnitude of the dataset is determined by the slice thickness and the reconstruction index and not by the number of CT detectors. Therefore, the number of images does not necessarily increase with the use of CT systems with more detectors. Scrolling through the dataset is helpful to identify and follow the pulmonary arteries, to identify pulmonary emboli and to differentiate between pulmonary arteries and other pulmonary structures. Thorough knowledge of the anatomy of the pulmonary arterial tree and the hilar structures and a systematic approach are essential for optimal interpretation. One possible and in our view useful and practical approach is to start with the pulmonary trunk and follow per lobe every artery from its origin to the periphery.

3.4 Multiplanar and curved reformats

With MDCT isotropic 3D datasets are obtained that allow for reconstruction in different directions without distortion or step-artefacts that are inherent to non-isotropic datasets obtained with SDCT or MDCT scanners below 16 detector rows.

While axial slices represent the base to evaluate a CTPA examination, additional reconstructions such as MPR's or curved planar reformats (CPR's), i.e., along the long axis of the vessel of interest and perpendicular to its lumen, are used as problem-solving tools: these reconstructions are helpful for the assessment of pulmonary arteries that are oriented oblique or parallel to the imaging plane, to distinguish central clots from perivascular lymphatic tissue, and to differentiate pulsation artefacts from real thrombi. Findings at MPR or other processing techniques should always be verified and correlated with findings in the axial plane.

MPR's represent the simplest and most frequently used processing technique. To obtain a good quality MPR, the slice thickness is usually 2 mm. MPR's can be reconstructed in any direction and the optimal direction is dependent on the patient's vascular anatomy and the individual findings and therefore should be done individually and not in a standardized way. Some vendors offer point-related MPR's in all three directions on demand: given a focal intravascular inhomogeneity that requires further attention, this particular area of interest will be automatically displayed in all three directions on demand allowing for analysis of the vascular inhomogeneity in the long as well as short axis of the vessel.

3.5 Maximum intensity projections

Maximum intensity projections (MIP's) are an excellent tool to obtain angiography-like images. As MPR's they can also be reconstructed in every direction. Since MIPs use 3D information, they show in opposite to MPRs the vessel to a longer extent. Sliding thin slab MIP's (3-5 mm thickness, with a maximum of 10 mm) were found to improve delineation of small peripheral vessels. Small peripheral thrombi will appear as less enhanced vessel segments with a lower density as compared to neighboring vessels with the same size. The use of MIP's is therefore recommended in every patient in which the initial standard axial reconstructions did not reveal PE.

The most important pitfall using MIP reconstructions refers to small hypodense structures (i.e., endovascular thrombi) that might be obscured by surrounding hyperdense structures (dense contrast-enhanced vessels). This occurs when MIP's slab thickness is too high or the display window is too narrow resulting in a too small contrast range. Choosing sufficiently thin slabs and adapting the window settings is therefore important.

Also MIPs represent an instantaneous feature on all dedicated and in our days most PACS workstations. MIP thickness and direction can be adapted on-line.

3.6 Computer aided diagnosis

The meticulous review of up to 300-500 axial images per CTPA study is a rather time-consuming task that requires a high level of attentiveness of the readers. While the majority of scans is made to exclude PE, the chance of missing small emboli increases with time pressure, anatomic and technical complexity and decreasing readers' experience (54).

CAD algorithms (figure 5) have been therefore developed to improve the detection performance of observers, to decrease interobserver variability and eventually to decrease reading time. None of the CAD algorithms for the detection of PE is currently FDA approved, and experience so far is therefore limited to scientific evaluation and study results.

Publications report an improved detection rate of small segmental and subsegmental emboli.

While CAD seems to be of no use in patients with multiple, central and rather obvious emboli, it may help especially inexperienced readers to detect small peripheral emboli which are seen in only a subset of patients and whose clinical relevance is still under debate. The number of false positive calls by the CAD algorithm is strongly related to image quality (figure 5) and may increase to more than 30 false positive calls in patients with a low enhancement or serious movement artefacts which undoubtedly is unpractical (55, 56). The majority of scans however have less than 5 false positive calls, which are quite easy to dismiss and therefore do not cause diagnostic problems. Use of CAD as "second reader" - meaning that CAD results are only used as additional information after having analyzed the scan first without CAD - inevitably leads to further increase of reading time. It is still under evaluation

whether CAD may be used more efficiently as "concurrent reader" meaning that already the initial reading process is supported by CAD candidates. In the future the automatic detection of vascular emboli may be also used for the quantification of thrombus load (57).

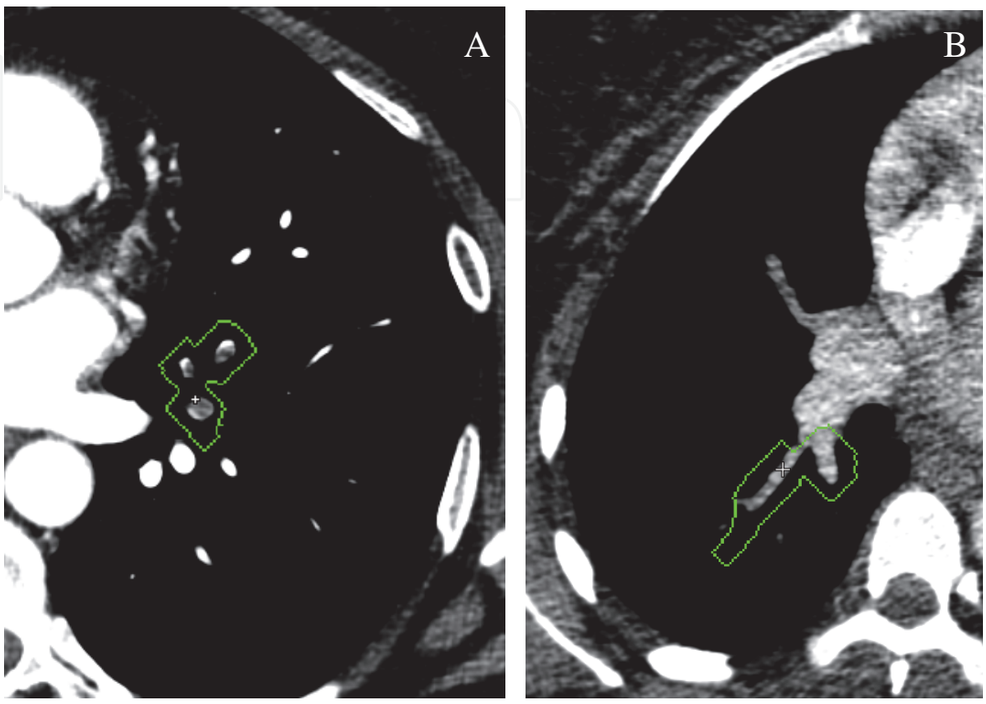

True positive candidate **False positive candidate**

Fig. 5. Automatic detection of pulmonary emboli using a CAD prototype (Philips Healthcare, the Netherlands): (A) example of true positive candidates, and (B) false positive candidates in badly opacified pulmonary arteries.

4. Imaging characteristics of PE

For correct interpretation of a CTPA study, every single artery from the main PA to the subsegmental branches has to be examined for signs of acute or chronic PE. Not only knowledge of the direct and indirect imaging characteristics of PE is essential, also familiarity with the pitfalls of the interpretation of the scan is required. Therefore the imaging characteristics of both acute and chronic PE will be outlined first followed by an overview of pitfalls related to technique, anatomy and patient.

4.1 Findings in acute PE

Direct signs of acute PE (figures 1, 4, 6-8) adapted and modified from the original description by Sinner (58), can be identified as:

a. a complete intraluminal filling defect caused by thrombus occluding the entire vessel lumen, potentially leading to a diameter enlargement of the affected artery compared to other pulmonary arteries of the same order of branching,

b. a partial filling defect centrally located in the vessel lumen caused by a clot surrounded by contrast medium: the finding is also named 'polo mint sign' when seen in cross section or 'railway track sign' when imaged along the long axis of the vessel, or
c. an eccentric partial filling defect that makes an acute angle with the PA wall caused by a mural thrombus that is outlined by contrast material (59-62).

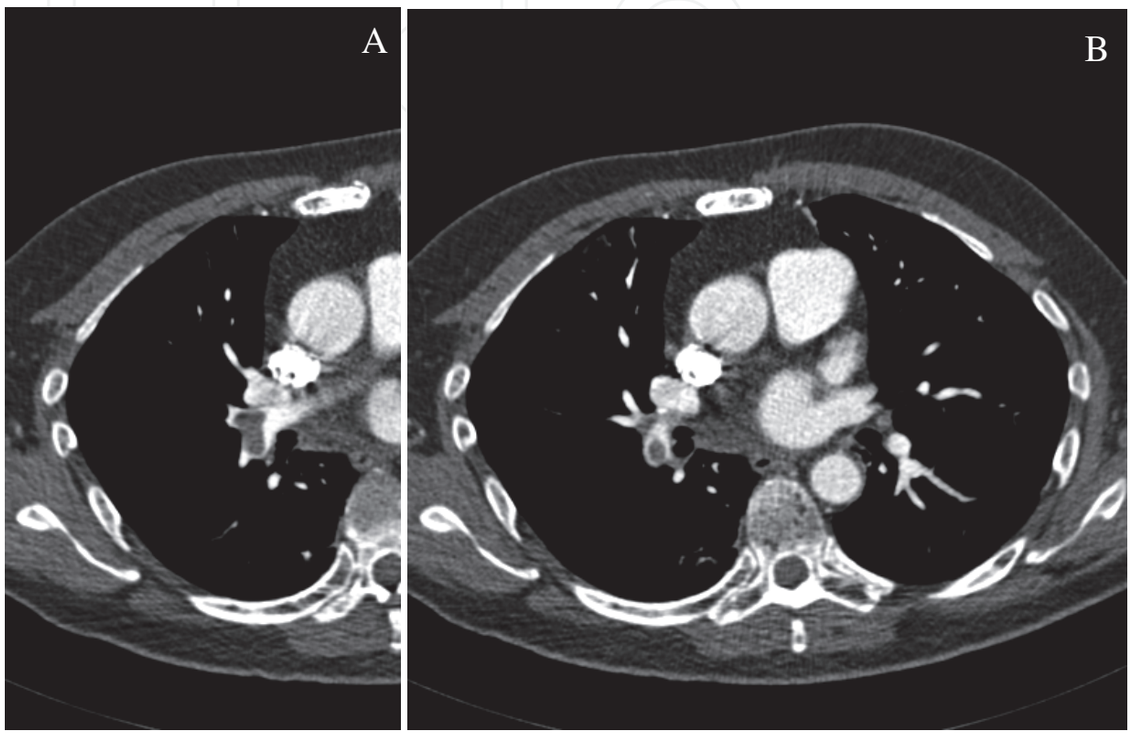

Fig. 6. Examples of direct and indirect signs of acute PE: centrally located non-obstructing thrombus, branching over the bifurcation of a pulmonary vessel, with acute angles to the vessel wall (A); centrally located partial filling defect ('doughnut or polo mint sign') with diameter enlargement as compared to the opposite side (B).

Several ancillary findings can be seen in patients with PE, but most of these are non-specific as they are seen also in other conditions. Wedge-shaped pleural-based consolidations and linear bands have shown to be statistically significantly related to PE (63). A peripheral wegde-shaped consolidation, typically without an air bronchogram, is likely to represent pulmonary infarction (figure 7) potentially with secondary haemorrhage. This is rarely encountered in healthy individuals because the bronchial artery collateral circulation will take over the blood flow to the embolized area. Other indirect findings include pleural effusions (figure 7) and atelectasis that are usually small, both quite frequently seen but non-specific signs. A mosaic perfusion pattern, caused by focal areas of hypoperfusion due to acute obstruction of blood flow through one or more pulmonary arteries, is more often seen on angiography than on computed tomography pulmonary angiography (CTPA) (64).
Although these indirect findings are considered to be of limited diagnostic value, they may suggest further investigations in case of an inconclusive CTPA.

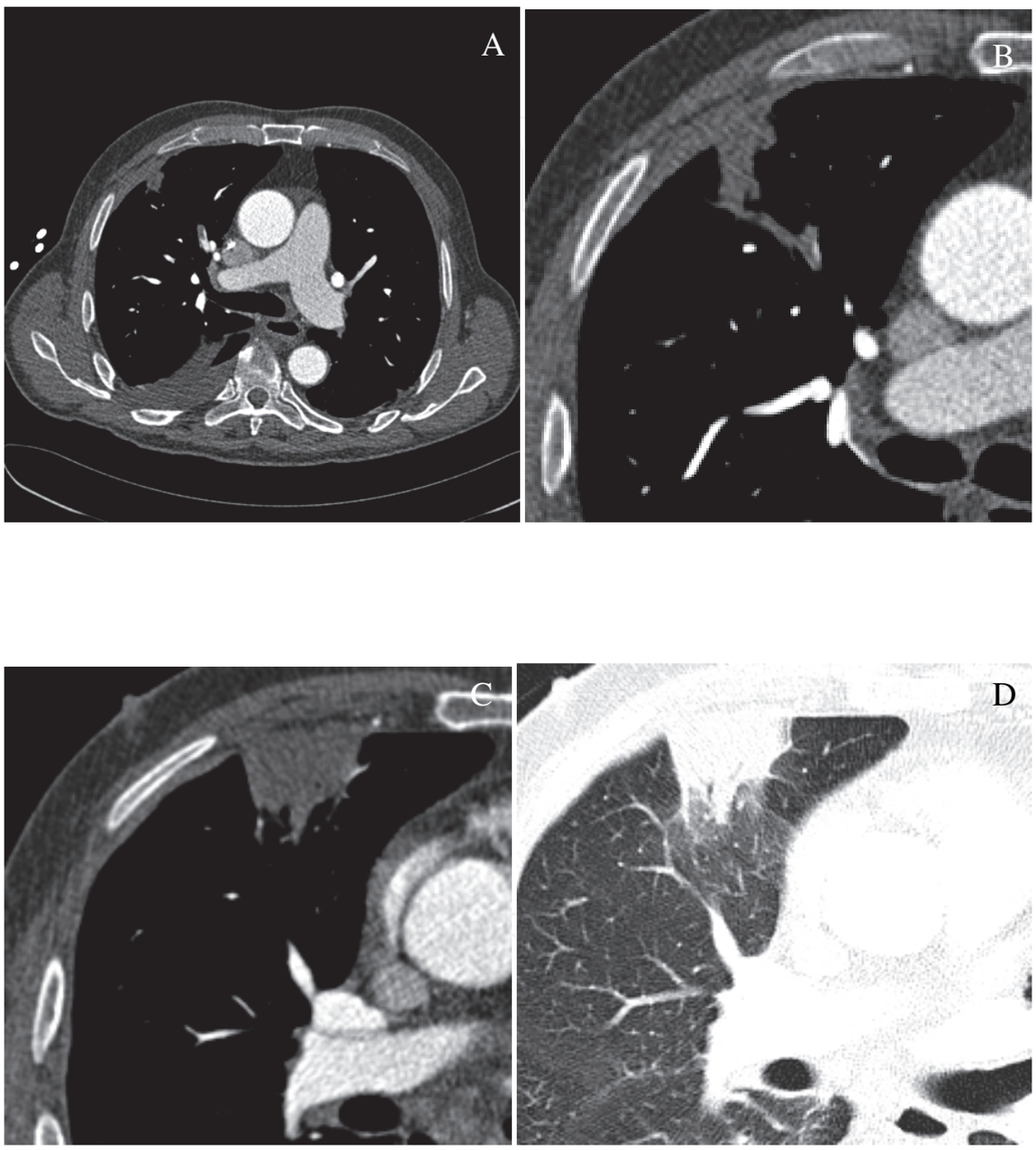

Fig. 7. Complete obstruction of a subsegmental pulmonary artery (A-C) with a wedge-shaped pleural-based consolidation (D) indicating a pulmonary infarction. A small pleural effusion is also present.

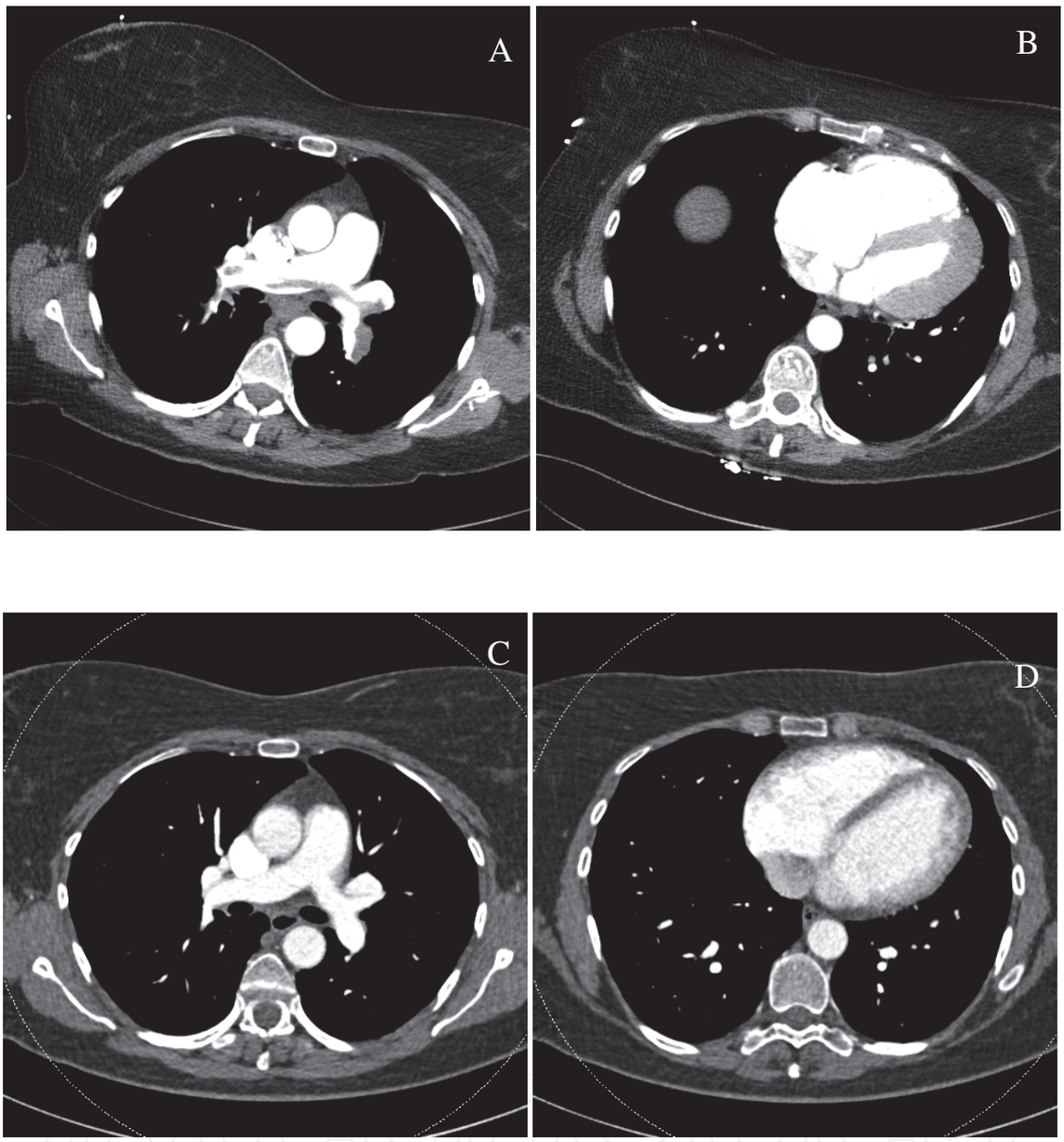

Fig. 8. CTPA of a 42-year-old female patient who presented with acute chest pain and hypotension revealed extensive central pulmonary emboli in combination with dilatation of the main PA (A) and the right ventricle (B). A follow-up scan after thrombolysis and 6 months of anticoagulant treatment revealed diameter normalization of the main PA (C) and the right ventricle (D). No residual thrombus was found.

4.2 Findings in chronic PE

Chronic PE has several imaging characteristics on a CTPA (figures 9-12), which correspond to imaging findings known from conventional pulmonary angiography. It can be identified as:

a. a complete intraluminal filling defect of a PA that is *smaller* than the adjacent patent pulmonary arteries,

b. an eccentrically located partial intraluminal filling defect that makes an obtuse angle with the PA wall,
c. an abrupt vessel narrowing often due to recanalization after complete occlusion by thrombus,
d. an apparently thick-walled artery, sometimes with irregular contours with irregularly narrowed lumen after recanalization
e. webs or bands visible in the arterial lumen,
f. partial or complete obstruction organizing with a concave configuration, with or without the appearance of distal pulmonary arteries on sequential scanning (65)
g. an intraluminal filling defect with the morphology of an acute PE present for more than 3 months (64, 66-68).

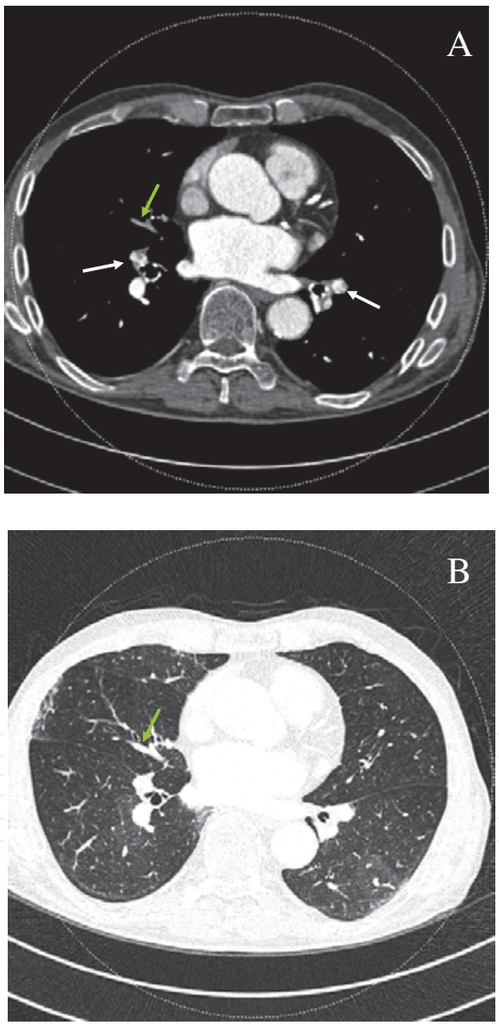

Fig. 9. Chronic PE in a 72-year-old male patient. CTPA with 1-mm axial reconstruction demonstrating bilateral eccentric thrombi with both acute and obtuse angles to the vessel wall (A, white arrows). A non-opacified vessel on the right side was (green arrow) found not to be accompanied by a bronchus on the pulmonary window setting (B), which is in agreement with a pulmonary vein. In addition, mosaic perfusion is present due to the chronic PE.

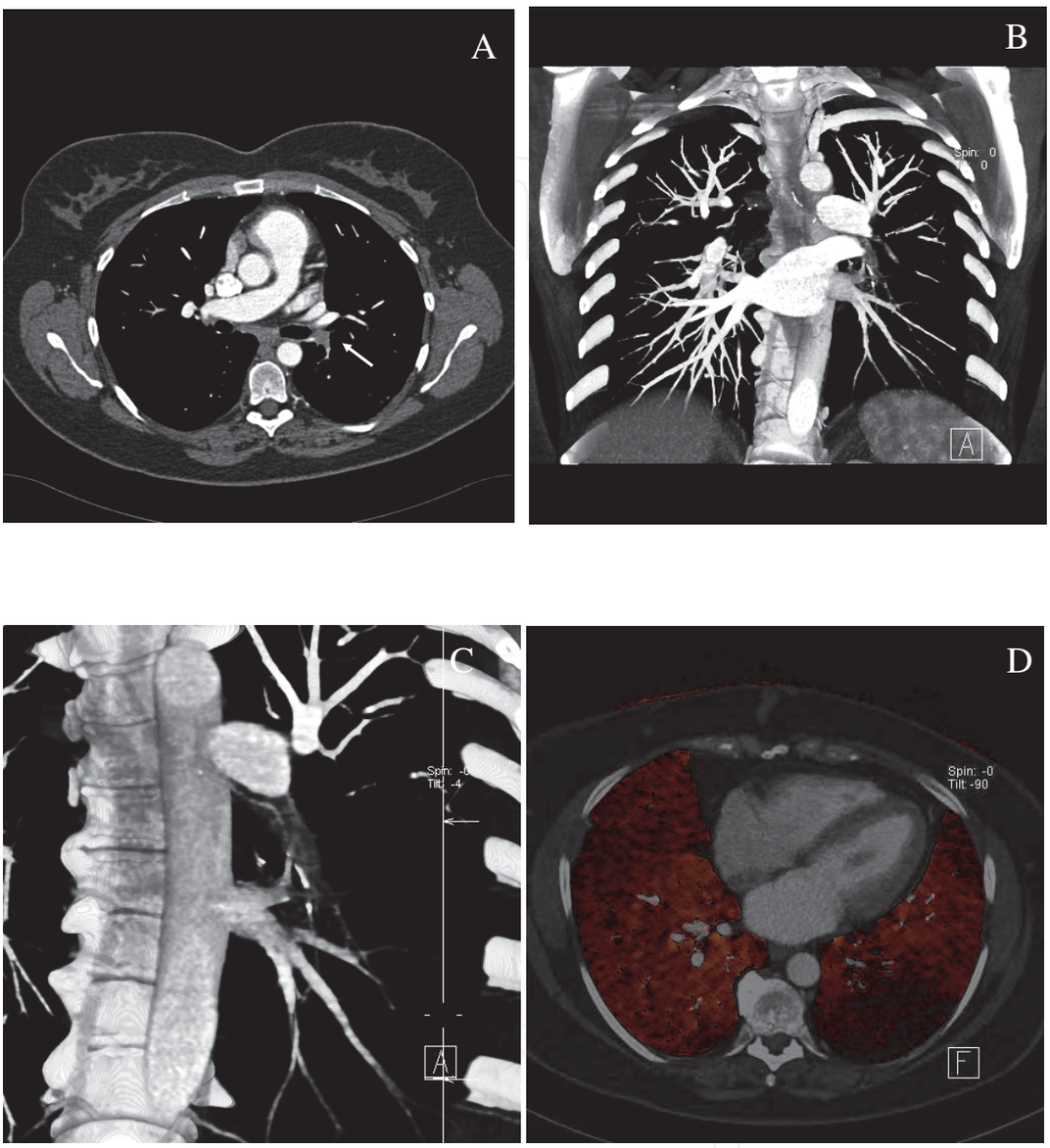

Fig. 10. Fifty-year-old female patient with complete obstruction of the left lower lobe PA due to chronic PE. Several CTPA scans were obtained for both follow-up and recurrent dyspnea. Complete obliteration and decreased diameter of the left lower lobe PA is demonstrated at 1-mm axial reconstruction performed using a single-source CT scanner (A, white arrow) and at additional coronal thin MIP reconstructions (B and C, detail). A fused color-coded and virtual 120 kV axial image demonstrates decreased perfusion in the left lower lobe (D, black area).

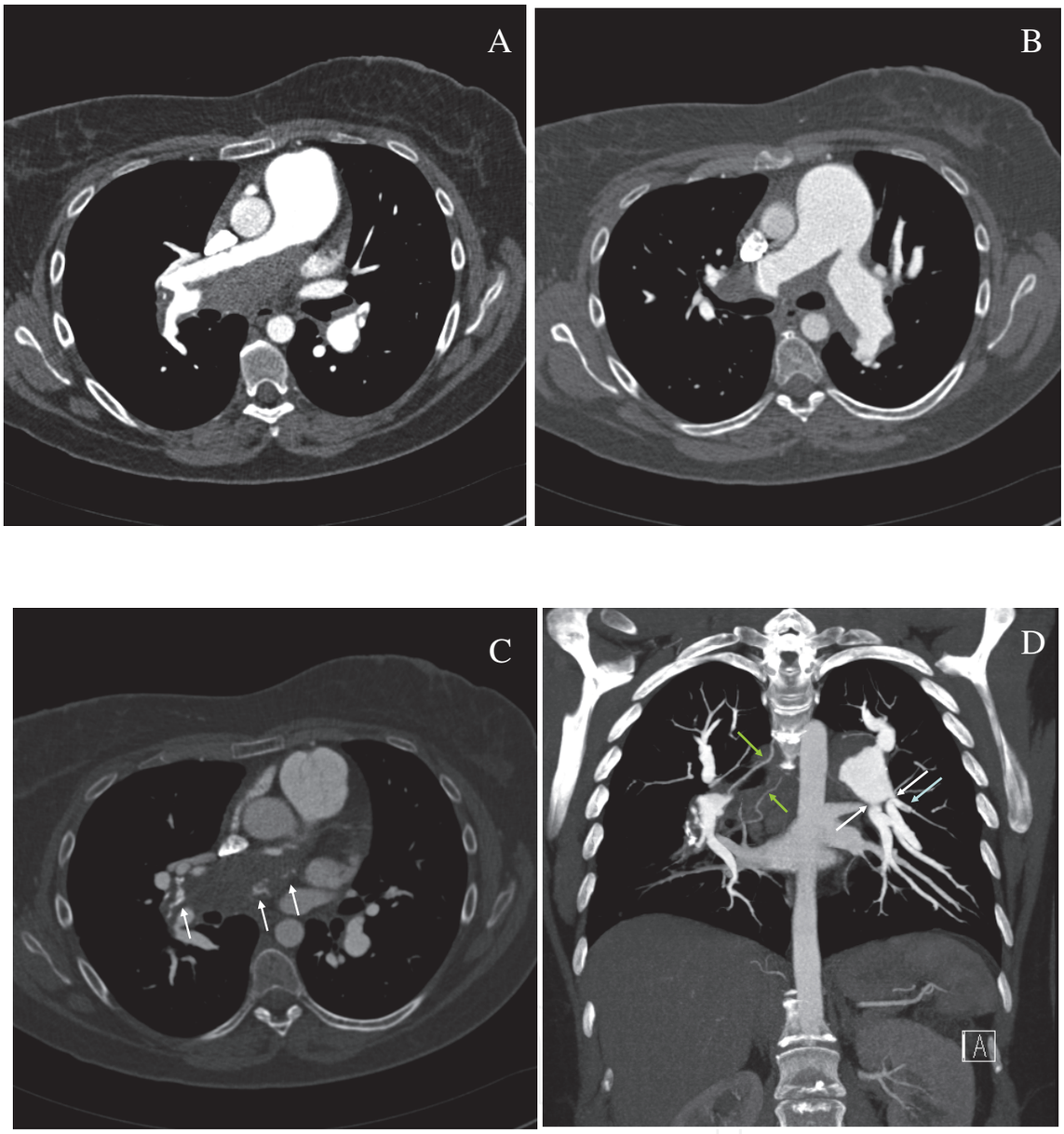

Fig. 11. Forty-year-old female patient with chronic thrombo-embolic PH. CTPA shows extensive eccentric thrombus with irregular contours of the inner surface in the right (A) and left (B) PA resembling a thick-walled PA. Calcifications (white arrows) in the thrombus are demonstrated with adaptation of the window settings (C). Coronal MIP reconstruction (D) demonstrates webs (white arrows), a small intraluminal filling defect (blue arrow) and dilatation of the bronchial arteries (green arrows) secondary to the chronic PE. The marked increase in diameter of the central pulmonary arteries (A and B) and the tortuosity of the pulmonary arteries (C) are indicative of PH.

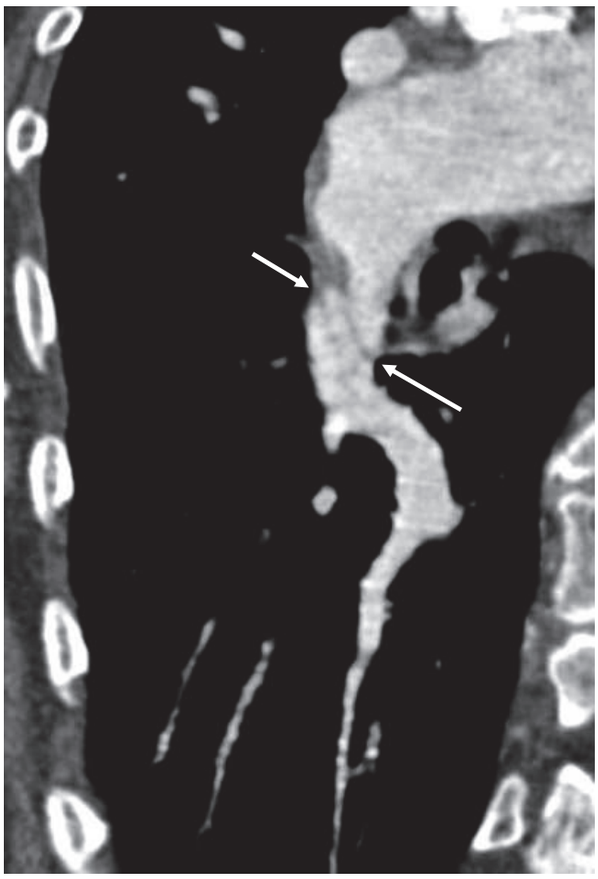

Fig. 12. Curved planar reformat of the right lower lobe PA in a patient with chronic PE demonstrates an intrapulmonary web (arrows).

At conventional pulmonary angiography, post-stenotic dilatation or aneurysm has been described in the setting of chronic PE in combination with the above findings (65).
Calcifications can be seen within the chronic thrombi in a small number of patients though it requires adaptation (widening) of the window settings in such a way that the calcifications are not obscured by the contrast material. Calcified thrombi in the subsegmental or smaller branches are often indistinguishable from small lung parenchymal calcifications, however their microtubular shape and position at the site of arterial branching may be helpful in the differential diagnosis (67).
A relatively common and serious complication of chronic PE is secondary PH, having an incidence of approximately 4 percent in the first two years after the first episode of PE (69). Therefore specific attention has to be paid to CT signs related to PH such as dilatation of the main PA (diameter more than 29 mm) (70), tortuous pulmonary vessels (71), hypertrophic bronchial arteries (72) a mosaic pattern and of lung attenuation due to variable perfusion. Mosaic pattern and the presence of systemic collateral supply are helpful signs to differentiate primary from secondary PH which has therapeutic implications (72, 73). In patients with recurrent PE, both chronic and acute PE can be present (figure 13).

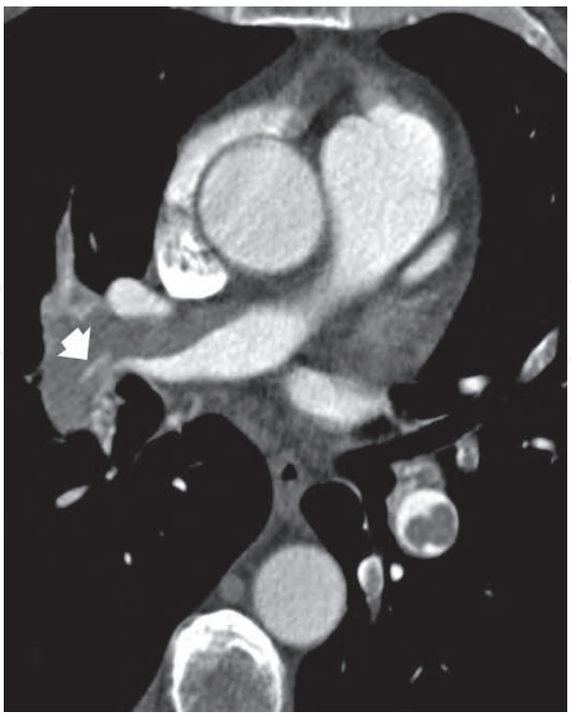

Fig. 13. Axial 1-mm thin slice demonstrating acute PE on the left side whereas on the right side a large centrally located eccentric thrombus is present with contrast in the thrombus as a result of recanalization (white arrow).

5. Pitfalls

To obtain an adequate interpretation of a CTPA the radiologist should be familiar with the various diagnostic pitfalls that can occur. Pitfalls can be divided into three groups dependant on their underlying cause we differentiate pitfalls related to technique, anatomy or patient factors (table 4).

Technique	Motion artefact Suboptimal contrast injection technique Partial volume effect Image noise Window settings Lung algorithm artefact Stair-step artefact
Anatomy	Pulmonary veins Hilar lymph nodes
Patient	Vascular abnormalities Mucus plugs PA sarcoma PA stump in situ thrombosis

Table 4. Pitfalls in the interpretation of CT of the pulmonary arteries.

5.1 Technique related pitfalls

5.1.1 Motion artefacts

One of the most common technique related pitfall is motion artefact, which is the major cause of an indeterminate CTPA (2). Respiratory and cardiac motion give rise to volume averaging of the vessel and surrounding lung parenchyma and can mimic a PE (figures 3 and 14) (62, 67). In addition, breathing can also result in inhomogeneous opacification of pulmonary arteries due to variations in the blood flow between inspiration and expiration, simulating an intraluminal filling defect (74).

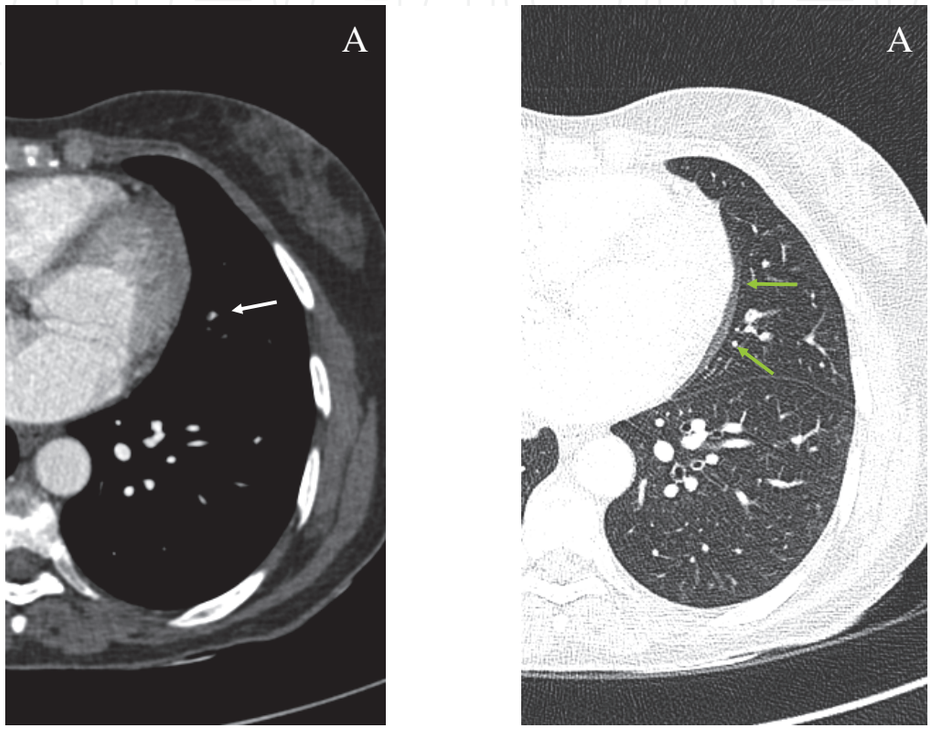

Fig. 14. Axial 1-mm slice showing a very small hypodense area in a small PA in the lingula (A, white arrow), which was due to a pulsation artefact as shown on the pulmonary window setting (B, green arrows).

Obvious motion can easily be detected by a rapid change in position and diameter on contiguous images or by observing the chest wall for respiratory motion during cine viewing of the images. When subtle, motion artifacts may be difficult to see on the mediastinal window settings, but can be clearly recognized on the lung window settings showing composite images of the vessels ('seagull sign') (62).

The rate of indeterminate studies due to motion artefacts has diminished with the introduction of multislice CT, since scanning times are reduced from 30 to 5-10 s, therefore requiring shorter breath holds. In a heavily dyspnoeic patient, image quality may be improved by limiting the scan range in z-direction e.g., to the range between superior contour of the aortic arch to the level of the inferior pulmonary veins, or by letting the patient gently breath during scan acquisition (59). A possibly artefact-free CTPA in an intubated patient can be achieved by suspending the ventilation in deep inspiration for the duration of the scan, which is possible in most sedated patients.

A disadvantage of the fast multislice CT scanners is that once a patient starts breathing during data acquisition, a relatively large scan volume might render indeterminate. Therefore gentle breathing during scanning may be preferred to deep inspiration in some patients, even though under these circumstances visualization and thus evaluation of peripheral small arteries is limited.

5.1.2 Suboptimal contrast injection technique

Another common pitfall related to scan technique is suboptimal contrast enhancement of the pulmonary arteries, due to inappropriate scan delay, flow rate or iodine concentration (22, 75, 76). Artefacts caused by improper scan delay are easily recognized because they typically result in appropriate vascular enhancement in the cranial or caudal part of the scan volume. Dependent on the extent of inappropriate vascular enhancement, a repeat examination with special focus on the suboptimally displayed anatomic area may be required.

A low flow rate can lead to poorly opacified pulmonary arteries especially at the level of the (sub)segmental arteries. The quality of enhancement of the small segmental and subsegmental arteries can be improved by using contrast material with a high iodine concentration. The disadvantage of high-contrast concentration, however, is streak artefacts at the level of the SVC (figure 15). Although these artefacts are readily identified by their radiating, poorly defined nature, as well as their usually non-anatomic configuration, they may create pseudo-filling defects in the right pulmonary and upper lobe arteries and may therefore render this part of the examination indeterminate.

Nowadays, to obtain optimal contrast enhancement in the pulmonary arteries high flow (4-6 ml/s) and high concentration (370-400 mg of iodine/ml) protocols are used in combination with a saline bolus injected immediately after the contrast bolus to reduce streak artefacts (19) (see also under 'injection protocol').

Fig. 15. CTPA of a 42-year-old male patient with acute chest pain 2 weeks after surgery revealing streak artefacts at the level of the right PA due to dense contrast in the SVC. No PE was found.

5.1.3 Partial volume effects

Small vessels that run parallel to the axis of the scan plane may simulate a PE by volume averaging with the surrounding lung parenchyma or adjacent bronchus (60, 62, 77). The arteries of the lingua and medial and lateral segments of the right middle lobe are particularly prone to such a volume averaging artefact. By using a thin collimation (< 2 mm) and multiplanar reformations the effects of volume averaging can be overcome enabling accurate analysis also of these vascular structures and thereby reducing false positive results.

5.1.4 Image noise

Especially in obese patients, image noise may substantially degrade image quality, and make the evaluation of the small segmental and subsegmental arteries very difficult if not even indeterminate. Although increasing the reconstruction width to 2.5 mm helps to decrease image noise and thereby improve signal-to-noise ratio and thus scan quality, it also decreases the sensitivity for detecting small pulmonary emboli (62, 78).

5.1.5 Window settings

The standard mediastinal window settings (window width 300-450, window level 30-50) may not always be adequate in the detection of PE, because the dense contrast material may obscure an intravascular thrombus (77). Therefore a more individual window setting is preferred (see under 'windowing'). The use of these settings in combination with the standard mediastinal and lung parenchym window settings will help to improve diagnostic accuracy.

5.1.6 Lung algorithm artefact

When the pulmonary arteries are visualized with images that are calculated using a high spatial frequency reconstruction convolution kernel used to improve the depiction of pulmonary vessels, bronchi and interstitium with the lung window, a high attenuation rim around vertically orientated vessels may be observed, potentially mimicking a PE. Interpretation of these vessels with the soft tissue reconstruction algorithm is crucial as these will no longer reveal the intraluminal filling defect (59, 62).

5.1.7 Stair-step artefact

The stair-step artefact is defined as the presence of surface irregularity artefacts along the margins of the pulmonary vessels ranging from a minimal indentation of the vessel margin to an appearance that mimics a pair of steps when viewed in profile (79). On the axial images, particularly in the vessels that run perpendicular to the scan plane, it may simulate a filling defect on one single slice, while neither the previous nor the next slice show abnormalities (80). However, on coronal and sagittal reformatted images stair-step artefacts are typically seen as horizontal high and low attenuation lines crossing the PA. Factors that can reduce this artefact are a narrow collimation and overlapping reconstruction intervals. Moreover, the use of multidetector CT has significantly reduced these artefacts.

5.2 Anatomy related pitfalls

5.2.1 Normal bronchovascular anatomy

Familiarity with the normal bronchovascular anatomy is essential in the diagnosis of PE. Pulmonary arteries run adjacent to their accompanying bronchus, with the exception of the apical posterior segment of the left upper lobe and the lingular arteries, which may course

separately for a short distance before rejoining with their bronchus. Pulmonary veins course in the interlobular septa, are not accompanied by a bronchus (figure 9) and can be followed towards the left atrium. By verifying their position and following their course on contiguous sections, a true arterial embolus can easily be distinguished from a pseudofilling defect in a pulmonary vein, the latter mostly due to flow artefacts or slow flow.
A vascular bifurcation can be misinterpreted as a web or band on the axial images. Coronal and sagittal reconstructions are helpful to reveal the true nature of this linear filling defect.

5.2.2 Hilar lymph nodes

The normal hilar lymph nodes are small, usually less than 3 mm, hypoattenuating, triangular or linear structures that follow the borders of the bronchovascular interstitium and are thus located in close proximity to the pulmonary arteries and bronchi (81). They can be divided into four groups in the right lung (i.e. the upper lobe, interlobar, middle and lower lobe groups) and four groups in the left lung (i.e. the culminal, interlobar, lingular and lower lobe groups) (81, 82). Knowledge of their size and location is important as they are a potential cause of a false positive diagnosis of PE. A small detector width and coronal and sagittal reconstructions can help distinguish them from a thrombus, showing their extramural location and the preservation of the smooth contour of the contrast-filled artery.

5.3 Patient related pitfalls

5.3.1 Vascular abnormalities

Asymmetric opacification of the pulmonary arteries can be caused by a unilateral increase in pulmonary vascular pressure, for example due to consolidation, atelectasis or pleural fluid, resulting in decreased flow in the ipsilateral arteries. Furthermore, absent or faint enhancement can be the result from unilateral obstruction of a main PA, or from unilateral shunting of blood from the systemic into the pulmonary circulation (74, 77). Left-to-right shunts can be due to the presence of intracardiac shunts, but most commonly they are encountered in patients with acquired disorders, particularly in chronic inflammatory diseases like bronchiectasis, in which a prominent bronchopulmonary circulation may exist. Retrograde flow of unopacified systemic blood from the bronchial arteries into the enhanced pulmonary arteries may potentially simulate a PE. Right-to-left shunting can arise in patients with a patent foramen ovale (PFO) if the pressure in the right atrium exceeds the left atrial pressure. This is a transient physiologic response during deep inspiration, Valsalva manoeuvre or coughing, but is a more persistent situation in cases of PE or PH (83). During CTPA this frequently leads to insufficient attenuation of the pulmonary arteries in combination with early and strong enhancement of the aorta, thereby limiting the diagnosis of PE.

5.3.2 Mucus plugs

Bronchi impacted with mucoid can be misinterpreted by an inexperienced reader as a PE. However, the observation of the contrast enhanced artery immediately adjacent to the apparent filling defect and the visualisation of normal bronchus proximally or distally on contiguous images on the lung window settings will easily reveal the nature of the tubular structure as a bronchus (62).

5.3.3 PA sarcoma

A sarcoma arising from the PA is a very rare lesion, which can be difficult to differentiate from acute or chronic PE. Knowledge of some distinguishing features is therefore important

(84, 85). In PA sarcoma the filling defect frequently spans the entire luminal diameter of the main or proximal PA, a finding which is unusual in PE. Moreover, vascular distension of the involved PA and local extravascular spread are other imaging characteristics that favour the diagnosis of a sarcoma. Late heterogeneous enhancement of the mass, due to neovascularity, necrosis, haemorrhage and occasionally calcifications, are sometimes observed. If a patient who was initially diagnosed as having a PE fails to respond to anticoagulant therapy, a PA sarcoma – though a rare occasion - should be considered.

5.3.4 PA stump in situ thrombosis

The incidence of PA stump thrombosis in patients who underwent pneumonectomy is approximately 12% (86, 87). Although local trauma of the vessel or the hypercoagulable state of blood in patients with a malignancy might contribute to the formation of the clot, the most important factor seems to be the stasis of blood flow, since the clot appears to be related to the length of the stump (86). Moreover, as it is often discovered as an incidental finding on routine follow-up CT and rarely shows other PA thrombi remote from the stump site, it is mostly considered a benign entity and not related to PE (87).

6. Summary

Since the introduction of spiral CT for the detection of PE, the continuous development of multi-detector technique and faster scanning lead to considerable improvement of image quality and visualization especially of smaller peripheral vascular structures. Though the overall percentage of non-diagnostic scans could be substantially improved, optimization of scan protocols, contrast administration and patient instruction remain crucial in order to obtain good quality scans. Inadequate vascular enhancement is still one of the most important causes for a non-diagnostic scan result. With scanning times of less than 5 s, a proper patient instruction has become even more important to avoid a Valsalva maneuver and breathing artefacts. Furthermore, the intravascular contrast can be optimized by lowering the kV and/or increasing the amount of iodine injected per s. With the development of the newer generation scanners the radiation dose can be substantially decreased. Further dose reduction is possible by reducing the scan range, reducing the kVp and using weight-adapted scan parameters. Special adaptations of the scan and contrast injection protocol are recommended in young patients and in pregnant women. In addition to the direct visualization of intravascular clots, indirect signs of acute PE may be helpful when image quality is suboptimal. An increased RV/LV ratio correlates well with PE severity and has been shown to be an independent predictor of an adverse outcome. The role of other CT parameters such as thrombus load as an independent predictor of outcome still needs to be determined.

With a DSCT scanner, lung perfusion can be directly visualized with potential additional functional information. CAD software packages have been developed in order to increase and harmonize diagnostic performance and decrease reading time. Though these new techniques are very promising, their value within the diagnostic algorithm for acute PE is not yet determined.

7. References

[1] Remy Jardin M, Remy J, Wattinne L, Giraud F. Central pulmonary thromboembolism: diagnosis with spiral volumetric CT with the single-breath-hold technique--comparison with pulmonary angiography. Radiology 1992; 185:381-387.

[2] Jones SE, Wittram C. The Indeterminate CT Pulmonary Angiogram: Imaging Characteristics and Patient Clinical Outcome. Radiology 2005; 237:329-337.
[3] Stein PD, Fowler SE, Goodman LR, et al. Multidetector Computed Tomography for Acute Pulmonary Embolism. N Engl J Med 2006; 354:2317-2327.
[4] Matsuoka S, Hunsaker AR, Gill RR, et al. Vascular Enhancement and Image Quality of MDCT Pulmonary Angiography in 400 Cases: Comparison of Standard and Low Kilovoltage Settings. Am. J. Roentgenol. 2009; 192:1651-1656.
[5] Szucs-Farkas Z, Kurmann L, Strautz T, Patak M, Vock P, ST. S. Patient exposure and image quality of low-dose pulmonary computed tomography angiography. Comparison of 100- and 80-kVp protocols. Invest Radiol 2008; 43:871-876.
[6] Heyer CM, Mohr PS, Lemburg SP, Peters SA, Nicolas V. Image Quality and Radiation Exposure at Pulmonary CT Angiography with 100- or 120-kVp Protocol: Prospective Randomized Study1. Radiology 2007; 245:577-583.
[7] Sigal-Cinqualbre AB, Hennequin R, Abada HT, Chen X, Paul J-Fo. Low-kilovoltage multi-detector row chest CT in adults: feasibility and effect on image quality and iodine dose. Radiology 2004; 231:169-174.
[8] Schueller-Weidekamm C, Schaefer-Prokop CM, Weber M, Herold CJ, Prokop M. CT Angiography of Pulmonary Arteries to Detect Pulmonary Embolism: Improvement of Vascular Enhancement with Low Kilovoltage Settings1. Radiology 2006; 241:899-907.
[9] Greess H, Wolf H, Baum U, et al. Dose reduction in computed tomography by attenuation-based online modulation of tube current: evaluation of six anatomical regions. Eur Radiol 2000; 10:391-394.
[10] Mastora I, Remy-Jardin M, Suess C, Scherf C, Guillot JP, Remy J. Dose reduction in spiral CT angiography of thoracic outlet syndrome by anatomically adapted tube current modulation. Eur.Radiol. 2001; 11:590-596.
[11] The 2007 roecommendations of the International Commission on Radiological Protection. ICRP publication 103. . Ann ICRP 2007; 37:1-332.
[12] European guidelines on quality criteria for computed tomography. Eur 16262 EN. . http://www.drs.dk/guidelines/ct/quality/htmlindex.htm
[13] Tack D, De Maertelaer V, Petit W, et al. Multi-Detector Row CT Pulmonary Angiography: Comparison of Standard-Dose and Simulated Low-Dose Techniques. Radiology 2005; 236:318-325.
[14] Schaefer Prokop C, Bankier A, Janata K, al. E. Complete chest CTA versus limited range CTA for the diagnosis of PE: what do we miss? ECR (abstract) 2005.
[15] Marten K, Engelke C, Obenauer S, Baum F, Grabbe E, Funke M. Diagnostic performance of retrospectively ECG-gated multislice CT of acute pulmonary embolism. [Diagnostischer Stellenwert der retrospektiven EKG-Triggerung in der mehrschicht-spiral-CT der akuten Lungenembolie]. Fortschr R”ntgenstr 2003; 175 1490-1495.
[16] White CS, Kuo D, Kelemen M, et al. Chest Pain Evaluation in the Emergency Department: Can MDCT Provide a Comprehensive Evaluation? American Journal of Roentgenology 2005; 185:533-540.
[17] Bae KT. Optimization of contrast enhancement in thoracic MDCT. Radiol.Clin.North Am. 2010; 48:9-29.
[18] Prokop M. Multislice CT angiography. Eur.J.Radiol. 2000; 36:86-96.
[19] Schoellnast H, Deutschmann HA, Fritz GA, Stessel U, Schaffler GJ, Tillich M. MDCT Angiography of the Pulmonary Arteries: Influence of Iodine Flow Concentration on

Vessel Attenuation and Visualization. American Journal of Roentgenology 2005; 184:1935-1939.

[20] Schoellnast H, Deutschmann HA, Berghold A, Fritz GA, Schaffler GJ, Tillich M. MDCT Angiography of the Pulmonary Arteries: Influence of Body Weight, Body Mass Index, and Scan Length on Arterial Enhancement at Different Iodine Flow Rates. In, 2006; 1074-1078.

[21] Bae KT, Tao C, GÃ¼rel S, et al. Effect of Patient Weight and Scanning Duration on Contrast Enhancement during Pulmonary Multidetector CT Angiography1. Radiology 2007; 242:582-589.

[22] Wittram C. How I Do It: CT Pulmonary Angiography. AJR Am.J.Roentgenol. 2007; 188:1255-1261.

[23] Haage P, Schmitz-Rode T, Hubner D, Piroth W, Gunther RW. Reduction of Contrast Material Dose and Artifacts by a Saline Flush Using a Double Power Injector in Helical CT of the Thorax. American Journal of Roentgenology 2000; 174:1049-1053.

[24] Coche EE, Hammer FD, Goffette PP. Demonstration of pulmonary embolism with dynamic gadolinium-enhanced spiral CT. Eur.Radiol. 2001; 11:2306-2309.

[25] Remy-Jardin M, Bahepar J, Lafitte J-J, et al. Multi-Detector Row CT Angiography of Pulmonary Circulation with Gadolinium-based Contrast Agents: Prospective Evaluation in 60 Patients1. Radiology 2006; 238:1022-1035.

[26] Gosselin MV, Rassner UA, Thieszen SL, Phillips J, Oki A. Contrast dynamics during CT pulmonary angiogram. J.Thorac.Imaging 2004; 19:1-7.

[27] Pontana F, Faivre J-B, Remy-Jardin M, et al. Lung Perfusion with Dual-energy Multidetector-row CT (MDCT): Feasibility for the Evaluation of Acute Pulmonary Embolism in 117 Consecutive Patients. Academic Radiology 2008; 15:1494-1504.

[28] Thieme SF, Johnson TRC, Lee C, et al. Dual-Energy CT for the Assessment of Contrast Material Distribution in the Pulmonary Parenchyma. Am. J. Roentgenol. 2009; 193:144-149.

[29] Fink C, Johnson TR, Michaely HJ, et al. Dual-Energy CT Angiography of the Lung in Patients with Suspected Pulmonary Embolism: Initial Results. Dual-Energy-CT-Angiografie der Lunge bei Patienten mit Verdacht auf Lungenembolie: Erste Ergebnisse 2008; 180:879-883.

[30] Zhang L-J, Chai X, Wu S-Y, et al. Detection of pulmonary embolism by dual energy CT: correlation with perfusion scintigraphy and histopathological findings in rabbits. European Radiology 2009; 19:2844-2854.

[31] Remy-Jardin M, Faivre J-B, Pontana F, et al. Thoracic Applications of Dual Energy. Radiologic clinics of North America; 48:193-205.

[32] Kerl JM, Bauer RW, Renker M, et al. Triphasic contrast injection improves evaluation of dual energy lung perfusion in pulmonary CT angiography. European Journal of Radiology 2010; In Press, Corrected Proof.

[33] Lu GM, Wu SY, Yeh BM, Zhang LJ. Dual-energy computed tomography in pulmonary embolism. Br J Radiol 2010; 83:707-718.

[34] Thieme SF, Becker CR, Hacker M, Nikolaou K, Reiser MF, Johnson TRC. Dual energy CT for the assessment of lung perfusion--Correlation to scintigraphy. European Journal of Radiology 2008; 68:369-374.

[35] Thieme SF, Graute V, Nikolaou K, et al. Dual Energy CT lung perfusion imaging--Correlation with SPECT/CT. European Journal of Radiology; In Press, Corrected Proof.

[36] Krissak R, Henzler T, Reichert M, Krauss B, Schoenberg SO, Fink C. Enhanced Visualization of Lung Vessels for Diagnosis of Pulmonary Embolism Using Dual Energy CT Angiography. Investigative Radiology 2010; 45:341-346.
[37] Remy-Jardin M, Pistolesi M, Goodman LR, et al. Management of Suspected Acute Pulmonary Embolism in the Era of CT Angiography: A Statement from the Fleischner Society1. Radiology 2007; 245:315-329.
[38] Matthews S. Imaging pulmonary embolism in pregnancy: what is the most appropriate imaging protocol? In, 2006; 441-444.
[39] Schuster ME, Fishman JE, Copeland JF, Hatabu H, Boiselle PM. Pulmonary Embolism in Pregnant Patients: A Survey of Practices and Policies for CT Pulmonary Angiography. In, 2003; 1495-1498.
[40] Boiselle PM, Reddy SS, Villas PA, Liu A, Seibyl JP. Pulmonary embolus in pregnant patients: survey of ventilation-perfusion imaging policies and practices. In, 1998; 201-206.
[41] van Beek EJR, Wild JM, Fink C, Moody AR, Kauczor H-U, Oudkerk M. MRI for the diagnosis of pulmonary embolism. Journal of Magnetic Resonance Imaging 2003; 18:627-640.
[42] International commission on radiological protection publication 84: pregnancy and medical radiation. Ann ICRP 2000; 30.
[43] Mallick S, Petkova D. Investigating suspected pulmonary embolism during pregnancy. Respiratory Medicine 2006; 100:1682-1687.
[44] Balan KK, Critchley M, Vedavathy KK, Smith ML, Vinjamuri S. The value of ventilation-perfusion imaging in pregnancy. In, 1997; 338-340.
[45] Nijkeuter M, Geleijns J, De Roos A, Meinders AE, Huisman MV. Diagnosing pulmonary embolism in pregnancy: rationalizing fetal radiation exposure in radiological procedures. Journal of Thrombosis and Haemostasis 2004; 2:1857-1858.
[46] Remy-Jardin M, Remy J. Spiral CT angiography of the pulmonary circulation. Radiology 1999; 212:615-636.
[47] Mabie W, DiSessa T, Crocker L, BM. S, KL. A. A longitudinal study of cardiac output in normal human pregnancy. Am J Obstet Gynecol 1994; 170:849-856.
[48] Wood KE. Major pulmonary embolism : review of a pathophysiologic approach to the golden hour of hemodynamically significant pulmonary embolism. Chest 2002; 121:877-905.
[49] Gibson N, Sohne M, Buller H. Prognostic value of echocardiography and spiral computed tomography in patients with pulmonary embolism. Current Opinion in Pulmonary Medicine 2005; 11:380-384.
[50] Bankier AA, Janata K, Fleischmann D, et al. Severity assessment of acute pulmonary embolism with spiral CT: evaluation of two modified angiographic scores and comparison with clinical data. J.Thorac.Imaging 1997; 12:150-158.
[51] Mastora I, Remy-Jardin M, Masson P, et al. Severity of acute pulmonary embolism: evaluation of a new spiral CT angiographic score in correlation with echocardiographic data. European Radiology 2003; 13:29-35.
[52] Qanadli SD, Hajjam ME, Vieillard-Baron A, et al. New CT index to quantify arterial obstruction in pulmonary embolism: comparison with angiographic index and echocardiography. AJR Am.J.Roentgenol. 2001; 176:1415-1420.
[53] Bae KT, Mody GN, Balfe DM, et al. CT Depiction of Pulmonary Emboli: Display Window Settings. Radiology 2005; 236:677-684.

[54] van Rossum AB, van Erkel AR, van Persijn van Meerten EL, Ton ER, Rebergen SA, Pattynama PMT. Accuracy of helical CT for acute pulmonary embolism: ROC analysis of observer performance related to clinical experience. Eur.Radiol. 1998; 8:1160-1164.

[55] Wittenberg R, Peters JF, Sonnemans JJ, Bipat S, Prokop M, Schaefer-Prokop CM. Impact of Image Quality on the Performance of Computer-Aided Detection of Pulmonary Embolism. In; 95-101.

[56] Dewailly M, Rémy-Jardin M, Duhamel A, et al. Computer-Aided Detection of Acute Pulmonary Embolism With 64-Slice Multi-Detector Row Computed Tomography: Impact of the Scanning Conditions and Overall Image Quality in the Detection of Peripheral Clots. Journal of Computer Assisted Tomography 2010; 34:23-30.

[57] Engelke C, Schmidt S, Auer F, Rummeny EJ, Marten K. Does computer-assisted detection of pulmonary emboli enhance severity assessment and risk stratification in acute pulmonary embolism? Clinical Radiology 2010; 65:137-144.

[58] Sinner W. Computed tomographic patterns of pulmonary thromboembolism and infarction. Journal of Computed Assisted Tomography 1978; 2:395-399.

[59] Ghaye B, Remy J, Remy-Jardin M. Non-traumatic thoracic emergencies: CT diagnosis of acute pulmonary embolism: the first 10 years. European Radiology 2002; 12:1886-1905.

[60] Kuzo RS, Goodman LR. CT evaluation of pulmonary embolism: technique and interpretation. AJR.Am.J.Roentgenol. 1997; 169:959-965.

[61] Remy-Jardin M, Remy J, Artaud D, Deschildre F, Fribourg M, Beregi J. Spiral CT of pulmonary embolism: technical considerations and interpretive pitfalls. Journal of Thoracic Imaging 1997; 12:103-117.

[62] Wittram C, Maher MM, Yoo AJ, Kalra MK, Shepard J-AO, McLoud TC. CT angiography of pulmonary embolism: diagnostic criteria and causes of misdiagnosis. Radiographics 2004; 24:1219-1238.

[63] Coche EE, MÃ¼ller NL, Kim KI, Wiggs BR, Mayo JR. Acute pulmonary embolism: ancillary findings at spiral CT. Radiology 1998; 207:753-758.

[64] Wittram C, Kalra MK, Maher MM, Greenfield A, McLoud TC, Shepard J-AO. Acute and Chronic Pulmonary Emboli: Angiography-CT Correlation. Am. J. Roentgenol. 2006; 186:S421-429.

[65] Auger WR, Fedullo PF, Moser KM, Buchbinder M, Peterson KL. Chronic major-vessel thromboembolic pulmonary artery obstruction: appearance at angiography. Radiology 1992; 182:393-398.

[66] Gottschalk A, Stein PD, Goodman LR, Sostman HD. Overview of prospective investigation of pulmonary embolism diagnosis II. Seminars in Nuclear Medicine 2002; 32:173-182.

[67] Remy-Jardin M, Mastora I, Remy J. Pulmonary embolus imaging with multislice CT. Radiologic Clinics of North America 2003; 41:507-519.

[68] Wittram C, Maher MM, Halpern EF, Shepard J-AO. Attenuation of Acute and Chronic Pulmonary Emboli1. Radiology 2005; 235:1050-1054.

[69] Pengo V, Lensing AWA, Prins MH, et al. Incidence of Chronic Thromboembolic Pulmonary Hypertension after Pulmonary Embolism. New England Journal of Medicine 2004; 350:2257-2264.

[70] Tan RT, Kuzo R, Goodman LR, Siegel R, Haasler GB, Presberg KW. Utility of CT Scan Evaluation for Predicting Pulmonary Hypertension in Patients With Parenchymal Lung Disease. Chest 1998; 113:1250-1256.

[71] Tardivon A, Musset D, Maitre S, et al. Role of CT in chronic pulmonary embolism: comparison with pulmonary angiography. Journal of Computed Assisted Tomography 1993; 17:345-351.
[72] Remy-Jardin M, Duhamel A, Deken Vr, Bouaziz Nb, Dumont P, Remy J. Systemic Collateral Supply in Patients with Chronic Thromboembolic and Primary Pulmonary Hypertension: Assessment with Multiâ€"Detector Row Helical CT Angiography1. In, 2005; 274-281.
[73] Grosse C, Grosse A. CT Findings in Diseases Associated with Pulmonary Hypertension: A Current Review. Radiographics 2010; 30:1753-1777.
[74] Remy-Jardin M, Remy J, Artaud D, Fribourg M, Beregi J. Spiral CT of pulmonary embolism: diagnostic approach, interpretive pitfalls and current indications. European Radiology 1998; 8:1376-1390.
[75] Hansell DM. Spiral computed tomography and pulmonary embolism: current state. Clin.Radiol. 1997; 52:575-581.
[76] Remy Jardin M, Remy J, Artaud D, Deschildre F, Fribourg M, Beregi JP. Spiral CT of pulmonary embolism: technical considerations and interpretive pitfalls. J.Thorac.Imaging 1997; 12:103-117.
[77] Gotway MB, Patel RA, Webb WR. Helical CT for the evaluation of suspected acute pulmonary embolism: diagnostic pitfalls. J.Comput.Assist.Tomogr. 2000; 24:267-273.
[78] Schoepf UJ, Holzknecht N, Helmberger TK, et al. Subsegmental Pulmonary Emboli: Improved Detection with Thin-Collimation Multi--Detector Row Spiral CT. Radiology 2002; 222:483-490.
[79] Boiselle PM, Hasegawa I, Nishino M, Raptopoulos V, Hatabu H. Comparison of artifacts on coronal reformation and axial CT pulmonary angiography images using single-detector and 4- and 8-detector multidetector-row helical CT scanners. Acad.Radiol. 2005; 12:602-607.
[80] Aviram G, Levy G, Fishman JE, Blank A, Graif M. Pitfalls in the diagnosis of acute pulmonary embolism on spiral computer tomography. Current Problems in Diagnostic Radiology 2004; 33:74-84.
[81] Remy-Jardin M, Duyck P, Remy J, et al. Hilar lymph nodes: identification with spiral CT and histologic correlation. Radiology 1995; 196:387-394.
[82] Sone S, Higashihara T, Morimoto S, et al. CT anatomy of hilar lymphadenopathy. Am. J. Roentgenol. 1983; 140:887-892.
[83] Henk CB, Grampp S, Linnau KF, et al. Suspected Pulmonary Embolism: Enhancement of Pulmonary Arteries at Deep-Inspiration CT Angiographyâ€"Influence of Patent Foramen Ovale and Atrial-Septal Defect1. Radiology 2003; 226:749-755.
[84] Cox CE, et al. Pulmonary artery sarcomas: a review of clinical and radiologic features. Journal of Computed Assisted Tomography 1997; 21:750-755.
[85] Yi C, Lee K, Choe Y, Han D, Kwon O, Kim S. Computed tomography in pulmonary artery sarcoma: distinguishing features from pulmonary embolic disease. Journal of Computed Assisted Tomography 2004; 28:34-39.
[86] Kim SY, Seo JB, Chae EJ, et al. Filling Defect in a Pulmonary Arterial Stump on CT After Pneumonectomy: Radiologic and Clinical Significance. Am. J. Roentgenol. 2005; 185:985-988.
[87] Kwek BH, Wittram C. Postpneumonectomy Pulmonary Artery Stump Thrombosis: CT Features and Imaging Follow-up1. Radiology 2005; 237:338-341.

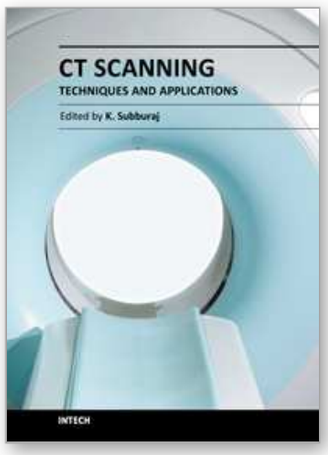

CT Scanning - Techniques and Applications

Edited by Dr. Karupppasamy Subburaj

ISBN 978-953-307-943-1
Hard cover, 348 pages
Publisher InTech
Published online 30, September, 2011
Published in print edition September, 2011

Since its introduction in 1972, X-ray computed tomography (CT) has evolved into an essential diagnostic imaging tool for a continually increasing variety of clinical applications. The goal of this book was not simply to summarize currently available CT imaging techniques but also to provide clinical perspectives, advances in hybrid technologies, new applications other than medicine and an outlook on future developments. Major experts in this growing field contributed to this book, which is geared to radiologists, orthopedic surgeons, engineers, and clinical and basic researchers. We believe that CT scanning is an effective and essential tools in treatment planning, basic understanding of physiology, and and tackling the ever-increasing challenge of diagnosis in our society.

How to reference

In order to correctly reference this scholarly work, feel free to copy and paste the following:

IJC Hartmann, PJ Abrahams-van Doorn and C Schaefer-Prokop (2011). State-of-the-Art Multi-Detector CT Angiography in Acute Pulmonary Embolism: Technique, Interpretation and Future Perspectives, CT Scanning - Techniques and Applications, Dr. Karupppasamy Subburaj (Ed.), ISBN: 978-953-307-943-1, InTech, Available from: http://www.intechopen.com/books/ct-scanning-techniques-and-applications/state-of-the-art-multi-detector-ct-angiography-in-acute-pulmonary-embolism-technique-interpretation-

INTECH
open science | open minds

InTech Europe
University Campus STeP Ri
Slavka Krautzeka 83/A
51000 Rijeka, Croatia
Phone: +385 (51) 770 447
Fax: +385 (51) 686 166
www.intechopen.com

InTech China
Unit 405, Office Block, Hotel Equatorial Shanghai
No.65, Yan An Road (West), Shanghai, 200040, China
中国上海市延安西路65号上海国际贵都大饭店办公楼405单元
Phone: +86-21-62489820
Fax: +86-21-62489821

IntechOpen